DEGRADATIVE PROPERTIES AND CYTOCOMPATIBILITY OF A MIXED-MODE HYDROGEL CONTAINING OLIGO[POLY(ETHYLENE GLYCOL) FUMARATE] AND THIOL-POLY(ETHYLENE GLYCOL)-THIOL

A Thesis
Presented to
The Academic Faculty

by

Kelly Sinclair Brink

In Partial Fulfillment
of the Requirements for the Degree
Master of Science in Biomedical Engineering

Georgia Institute of Technology

May 2008

DEGRADATIVE PROPERTIES AND CYTOCOMPATIBILITY OF A MIXED-MODE HYDROGEL CONTAINING OLIGO[POLY(ETHYLENE GLYCOL) FUMARATE] AND THIOL-POLY(ETHYLENE GLYCOL)-THIOL

Approved by:

Dr. Johnna S. Temenoff, Advisor
Wallace H. Coulter Department of Biomedical Engineering
Georgia Institute of Technology

Dr. Andrés J. García
School of Mechanical Engineering
Georgia Institute of Technology

Dr. Marc E. Levenston
Department of Mechanical Engineering
Stanford University

Dr. Ravi V. Bellamkonda
Wallace H. Coulter Department of Biomedical Engineering
Georgia Institute of Technology

Date Approved:
Wednesday March 19th, 2008

To my parents and sister for their unconditional love and support.

ACKNOWLEDGEMENTS

I wish to thank those persons who have assisted with various aspects of this thesis project, including Mr. Johnafel Crowe and my peers in the Temenoff Laboratory for their support.

TABLE OF CONTENTS

LIST OF TABLES

LIST OF FIGURES

SUMMARY

Knee injuries are a major cause of orthopedic disabilities in the United States, with over 9.5 million people visiting orthopedic surgeons for knee related injuries in 2003. Current reconstruction techniques for torn anterior cruciate ligaments (ACL) require extensive surgery and long physical rehabilitation times since the tissue does not heal upon injury. A common ACL injury occurs where the gap at the rupture site remains open after injury and fails to heal, which can lead to premature osteoarthritis and disability. Hydrogels are a popular material used for tissue engineering applications due to their ability to retain water and good biocompatibility. Previous work has shown that hydrogels or bio-functionalized polymers can be made through the mixed-mode reaction of radically crosslinked thiol groups and acrylate end groups. This project explores mixed-mode oligo[poly(ethylene glycol) fumarate] (OPF)-based hydrogels as alternate carriers for regeneration of partial tear ligament defects. The main purpose of this thesis project was to determine the degradative properties of and cell response to thiol-PEG-thiol (PEG-diSH), a novel hydrogel material. The swelling and degradative properties of hydrogels containing three components – OPF, PEG-diacrylate (PEG-DA), and PEG-diSH were characterized by their fold swelling. In addition, cell viability, morphology changes, proliferation and collagen production were analyzed in tri-ratio hydrogels with and without the presence of RGD over three weeks.

Results showed that the hydrogels containing PEG-diSH demonstrated significantly larger fold swelling and promoted cell clustering (as shown by increased area of clusters), probably due to the larger mesh size and possibly due to the presence of

free thiol functional groups present in the network from the mixed-mode reaction. However, an increase in cell number was not found in these gels up to eight days, suggesting that cell migration may play a role in the appearance of clusters. Additionally, increased cell spreading in response to RGD was observed inside gels containing PEG-diSH; no spreading was seen in the non PEG-diSH gels (± RGD), possibly because the mesh size was too small to allow for clustering or spreading within the matrix.

Results from this work suggest that the presence of PEG-diSH could promote cell-cell contact within the clusters which could be useful in systems where direct contact promotes tissue formation or cell differentiation.

CHAPTER 1

INTRODUCTION

Background

Hydrogels for Tissue Engineering

Tissue engineering (TE) was first proposed in the early 1990s as an alternative to organ transplantation that could be achieved using three strategies: isolated cell sources, addition of tissue-inducing cytokines and growth factors, and utilizing cells on or within matrices[1-3]. The type of scaffold used is important since it must maintain its mechanical strength, provide structural support, and provide the optimal growth environment for the cells. Hydrogels are a popular material used for TE applications due to their ability to retain water and good biocompatibility[4, 5]. They are composed of polymer networks that are insoluble in water and swell to an equilibrium volume while retaining their pre-swollen shapes[5]. The hydrogel networks generally have hydrophilic chemical residues within the polymer backbone, although it is possible to fabricate hydrogels that have a significant portion of hydrophobic residues by blending or co-polymerizing hydrophilic and hydrophobic polymers[5].

Hydrogels are insoluble in water due to the three-dimensional network and the equilibrium that exists between forces acting on the hydrated chains (dispersing) and forces preventing further penetration of water (cohesive)[5]. The cohesive forces are generated by covalent bonding between the polymer chains or by hydrophobic/Van der Waals forces and hydrogen bonding[5]. Hydrogels can be designed to swell or shrink when exposed to exogenous signals (temperature, pH, light, etc.)[6, 7] and can be fabricated from natural or synthetic polymers and be degradable or non-degradable[5]. Hydrogels can be

chemically polymerized (either thermal- or photo-initiated) if the polymer macromers have vinyl residues or physically cross-linked without chemical initiators (like chitosan, hyaluronan, and alginate)[5].

Ligament Tissue Engineering

Knee injuries are a major cause of orthopedic disabilities in the United States, with over 9.5 million people visiting orthopedic surgeons for knee related injuries in 2003[8]. The knee is an extremely active joint in the body and is prone to inflammation and tears, especially in athletes. Usually, knee ligaments are torn when the knee is forced to stop and change movement direction rapidly[8]. The anterior cruciate ligament (ACL) is the most frequently injured ligament[9] and approximately 75,000 ligament repair and reconstruction surgeries are performed annually[8]. Current ACL reconstruction techniques require extensive surgery and long physical rehabilitation times since the tissue does not heal upon injury. The preferred method for ligament reconstruction utilizes autografts from either patellar tendon or hamstring tendon since synthetic grafts encounter long-term failure as they are unable to replicate the mechanical properties and structural characteristics of native ACL tissue[10, 11]. Even so, autografts do not consistently integrate with the bone tissue and as a result never regain the full strength of the native tissue after implantation[12, 13]. Often, autografts result in tendonitis, arthritis, muscle atrophy, and donor site morbidity[11]. Therefore, orthopedic scientists and surgeons have been trying to research methods to repair and regenerate injured ligaments in joints through a variety of tissue engineering techniques.

The development of a functional tissue engineered ligament is based on the three components of TE mentioned above: an appropriate cell source, a structural scaffold, and an environment that provides sufficient nutrient transport and regulatory stimuli[14]. The scaffold may be seeded with cells and modified to enhance biocompatibility and stimulate cellular response and allow for cellular adhesion and proliferation[14]. The scaffold also must have initial mechanical strength, but then degrade over time to allow new tissue ingrowth. A variety of scaffolds have been investigated in regards to ligament TE, including collagen[15, 16], silk[17, 18], biodegradable polymers[19, 20], and natural hydrogels such as hyaluronic acid, chitosan, and alginate[21, 22].

A common ligament injury occurs in the ACL, where the gap at the rupture site remains open after injury and fails to heal, which can lead to premature osteoarthritis and disability[23, 24]. The inability of this gap to heal can be caused by the intra-articular environment of the ACL (particularly the presence of synovial fluid)[25-28], and by the mechanics of the ligament, including the twisting of the ligament in the knee joint and the load forces it experiences. One of the main research strategies used in animal models and clinically for repair of these gaps involves using fibrin clots to stimulate ligament repair[29-31]. Hydrogels being investigated for partial tear repair have been mainly made out of collagen to promote increased recruitment of growth factors associated with healing[23, 24, 32]. While most studies investigating partial ligament tears have focused on overcoming deficiencies in the cell sources chosen, very few have focused on the scaffolding required for successful repair[23]. The work presented in this thesis could provide a useful hydrogel system for investigating the effects of scaffold type on the repair of partial tears in ligaments.

Poly(ethylene glycol)-based Hydrogels and Thiol-Acrylate Systems

Poly(ethylene glycol) (PEG) is a common polymer used in tissue engineering applications due to its minimal toxicity when used in animals and humans. Many studies have used PEG-based hydrogels in cell culture studies and have shown that the PEG-derivatives are non-cytotoxic to a variety of cell types, including MSCs, osteoblasts, and fibroblasts[33-35]. A PEG-derivative, oligo[poly(ethylene glycol) fumarate] (OPF), was developed in the Mikos laboratory as an injectable cell carrier for orthopedic tissue engineering applications[36, 37]. OPF, when cross-linked with PEG-diacrylate (PEG-DA), has been shown to be non-cytotoxic to a variety of cell types[38, 39] and has been shown to have physical properties (mesh size, swelling characteristics) that can be tailored for specific tissue engineering applictions[40, 41].

PEG-based hydrogels that are crosslinked using a photo-initiating system have been studied extensively for cell encapsulation purposes[42-45]. The advantages of this type of radical polymerization system is the ability to both spatially and temporally control the reaction kinetics, uniformly encapsulate cells, and adapt the system for in situ polymerization[45]. The photoinitiator Irgacure 2959 (D2959) has been found to be non-toxic to cells and has been used in encapsulation of a variety of cell types, including osteoblasts, fibroblasts, and chondrocytes[46-48].

Previous work has shown that hydrogels can be made through the Michael-type addition reaction of thiol groups and acrylate end groups[49-58]. This coupling between these groups can be combined with a radically-initiated crosslinking reaction, creating a mixed-mode reaction scheme that produces a covalently crosslinked network[49]. This reaction combines the two types of polymerization schemes: step growth and chain

growth. In step growth polymerization, growing chains of any length can react with each other to form longer chains while in chain growth, monomers can only be added on to the growing polymer chains one at a time. In this system, initiation occurs through the photoinitiator, which produces a radical that reacts with a thiol functional group to produce a thiyl radical. The propagation starts with a thiol-ene step growth mechanism whereby the thiyl radical reacts with the vinyl functional group of the acrylate followed by chain transfer from the resulting carbon radical to a thiol functional group which regenerates the thiyl radical. However, homopolymerization of the acrylate groups must also be taken into account due to the ability of acrylate groups to react with carbon-based radicals. This additional chain-growth mechanism completes the mixed-mode scheme, which is impacted by thiol to acrylate ratios, transitioning from more chain like to more step like as the ratio of thiol to acrylate increases[56].

An important material property of hydrogels, degradation, has been achieved through hydrolytic cleavage of esters and anhydrides and through enzymatic cleavage of peptide sequences incorporated into the network[59, 60]. Hydrogels fabricated through the thiol-acrylate mixed-mode reaction scheme degrade hydrolytically at physiological pH through cleavage of ester linkages[49, 50, 61, 62]. Studies also found that the number of carbon atoms between the ester and sulfide groups influence the rate of ester hydrolysis (the closer the ester is to the sulfide group, the faster the network degrades)[55, 62].

Purpose of Thesis Project

This project explores mixed-mode OPF-based hydrogels as alternate carriers for regeneration of partial tear ligament defects. The purpose of this thesis project was to

determine the degradative properties of and cell response to thiol-PEG-thiol (PEG-diSH), a novel hydrogel material. The first goal of this thesis project was to characterize the swelling and degradative properties of hydrogels containing three components – OPF, PEG-diacrylate (PEG-DA), and PEG-diSH. Constructs containing varying ratios of these components were fabricated and their fold swelling after 24 hours was calculated to determine the effect of PEG-diSH on the swelling properties of hydrogels. Also, the effect of initial water percentage on the swelling properties of gels made from the same ratio of components was investigated. The degradative properties of hydrogels containing PEG-diSH were compared through fold swelling calculations over 30 days compared to hydrogels containing no PEG-diSH. We hypothesized that the incorporation of PEG-diSH into the hydrogel network would increase the mesh size of the hydrogels and therefore increase the swelling properties of OPF/PEG-DA hydrogels as well as influence the degradation parameters of the hydrogels.

The second goal of the project was to elucidate the effects of PEG-diSH incorporation into the hydrogels on the viability, cell morphology, proliferation, and collagen synthesis of ligament fibroblasts in the presence or absence of the RGD adhesion ligand. Constructs containing OPF, PEG-DA, and PEG-diSH were fabricated at two different initial water percentages to investigate the effect of the presence of water during polymerization on cell survival. Constructs were also fabricated with and without PEG-diSH and with and without the RGD adhesion ligand to determine the effect of the presence of PEG-diSH and RGD on the viability and morphology of encapsulated tendon/ligament fibroblasts. This study used viability analysis, image analysis, DNA and total collagen assays to elucidate the effects of PEG-diSH and RGD on the viability, cell

morphology, proliferation, and collagen synthesis of encapsulated cells. We hypothesized that the incorporation of PEG-diSH and RGD would influence cell viability and morphology due to the increase in mesh size of the gels and the interaction of the RGD ligand with cell surface receptors, and therefore stimulate proliferation and matrix production of encapsulated cells.

CHAPTER 2

MATERIALS AND METHODS

Hydrogel Fabrication

Oligo[poly(ethylene glycol) fumarate] (OPF) Synthesis and Characterization

Synthesis. Oligo[poly(ethylene glycol) fumarate] (OPF) was synthesized as previously reported[63]. Briefly, poly(ethylene glycol) (PEG; nominal MW = 10,000 Da, Sigma-Aldrich) was distilled and dissolved in dichloromethane (distilled before use) (Fisher Scientific) to produce a 40% (v/v) solution. The correct amounts of fumaryl chloride (FuCl; distilled before use, Sigma-Aldrich) and triethylamine (TEA; Sigma-Aldrich) for a molar ratio of 0.9 PEG:FuCl were added dropwise to the PEG solution and the reaction was held at approximately 0^{o}C and carried out under nitrogen. After the addition of FuCl and TEA, the OPF formulation was constantly stirred for another 24-72 hours at 25^{o}C to ensure the completion of the reaction. At this time, the excess dichloromethane was evaporated and the Cl-TEA salt was removed. The OPF was recrystallized twice in ethyl acetate (Fisher Scientific) and washed three times in ethyl ether (Fisher Scientific). The resulting powder was vacuum dried at < 5 mmHg and stored in a sealed container at -20^{o}C until further use.

Gel-permeation chromatography (GPC) and nuclear magnetic resonance spectroscopy (NMR). After synthesis, the OPF was characterized via GPC and NMR. A GPC system (Waters Model 410) equipped with a refractometer was used to determine the molecular weights of both the PEG used for synthesis and the resulting OPF polymer. The polymer samples were dissolved in chloroform, filtered (0.45 μm filter) and injected into a column (50 – 100,000 g/mol range; Waters) at a flow rate of 1 mL/min. Molecular

weights were determined from elution time based on a calibration curve generated from PEG standards (nine standards ranging in molecular weights from 194 - 71,000 Da; Waters). The samples were run in triplicate. In order to verify the addition of fumarate groups to the OPF, samples were dissolved in $CDCl_3$ and ^{1}H-NMR spectra were obtained with a Bruker Avance 400 MHz NMR system (Bruker Analytik).

Arg-Gly-Asp (RGD) Peptide Conjugation

For cell encapsulation experiments, the adhesion peptide GRGDS (Calbiochem) was functionalized by conjugating it to an acryloyl-PEG-*N*-hydroxysuccinimide spacer arm (Ac-PEG-NHS; M_n = 3400 Da, Nektar) to produce an acrylated peptide. The peptide and excess Ac-PEG-NHS were reacted in a sodium bicarbonate buffer (pH 8.3) under stirring at room temperature for 2.5 hours. The product was then dialyzed against dH_2O for two days to remove any unreacted peptide. The dialyzed Ac-PEG-RGD product was frozen in liquid nitrogen and lyophilized for two days and then stored at -20^{o}C until use.

Hydrogel Construct Fabrication

Hydrogel constructs were fabricated from OPF, the cross-linker PEG-diacrylate (PEG-DA; M_n = 3400 Da, Laysan Bio) and thiol-PEG-thiol (PEG-diSH; M_n = 3400 Da, Laysan Bio) in ratios by weight. The UV photo-initiator Irgacure 2959 (D2959; Ciba) was dissolved in *N*-vinyl pyrrolidone (NVP; Sigma-Aldrich) at a concentration of 0.05% D2959 (weight/total weight) in 10% NVP (weight/polymer weight). The polymers were dissolved in phosphate buffered saline (PBS) (pH 7.4) and the photo-initiator was introduced to the system. The polymer solution was placed in 6 mm diameter by 1 mm

thick Teflon molds (~30 μL) and polymerized under UV light (365 nm, 18 mW/cm^2) to create constructs (see Table 1 for polymerization times).

Swelling Characteristics

Hydrogels were fabricated as stated above (see Table 1 for specific formulations) and allowed to swell in PBS for twenty-four hours, at which point the wet weights were recorded. The constructs were then placed in Teflon lined Petri dishes and lyophilized for twenty-four hours. The dry weights were recorded and used to calculate the fold swelling of the hydrogels (wet weight/dry weight).

Degradative Properties

Hydrogel constructs were fabricated (see Table 1 for specific formulations) and allowed to swell in PBS for twenty-four hours, at which point the Day 1 wet and dry weights were recorded. At each successive timepoint in the study, the wet and dry weights were recorded and used to calculate fold swelling of the hydrogels.

Table 1. Hydrogel formulations for swelling and degradation studies.

Swelling Study #1 (60% initial water content)*		
Formulations (w/w/w) (n=4)		
OPF %	PEG-DA %	PEG-diSH %
40	60	0
40	30	30
50	50	0
50	25	25
60	40	0
60	20	20
polymerization time: 11 minutes		
Swelling Study #2 (60% and 75% initial water contents)		
Formulations (w/w/w) (n=3)		
OPF %	PEG-DA %	PEG-diSH %
60	20	20
60	40	0
polymerization time: 15 minutes		
Degradation Study (75% initial water content)		
Formulations (w/w/w) (n=4)		
OPF %	PEG-DA %	PEG-diSH %
60	20	20
60	30	10
60	40	0
polymerization time: 13 minutes		
* initial water content = weight of water/ total weight of the polymer solution before cross-linking		

Cell Encapsulation in Hydrogel Constructs

Cell Harvest and Isolation

Fibroblasts were isolated from the cruciate ligaments and patellar tendons of immature bovine knee joints (Research 87). Briefly, the excess tissue was removed and the joint capsule was transferred to the cell culture hood, where the ligaments and tendons were removed in a sterile fashion. The tissue was digested in a solution containing Dulbecco's Modified Eagle Medium (DMEM), 10 ml/L PSN, 10 ml/L kanamycin, 1 ml/L gentamicin, 1 ml/L fungizone, and 0.4% collagenase II (w/v) (Invitrogen) for forty-eight hours, at which point the solution was filtered through a cell

strainer with nylon mesh lining (80 μm pores; Small Parts, Inc). The solution was then centrifuged and the collagenase was removed. The cells were resuspended in DMEM, counted on a hemocytometer, and frozen down in DMEM containing 20% fetal bovine serum (FBS) and 10% dimethyl sulfoxide (DMSO). The cells were put into cryovials and frozen in a controlled-rate cooler at -80^{o}C and then transferred to liquid nitrogen for long-term storage.

Cell Culture

Tendon/ligament fibroblasts were thawed and plated at 2E6 cells/flask in growth medium containing DMEM, 10% FBS (Hyclone), 1% non-essential amino acids (NEAA; Mediatech), 1% HEPES (Mediatech), 0.1% gentamicin (Mediatech), 0.1% fungizone (Invitrogen), and 50 μg/mL ascorbate (Sigma-Aldrich). The media was changed one day after plating and every 2-3 days thereafter. The cells were grown to confluency and then lifted using 0.05% trypsin/EDTA for use in experiments.

Cell Encapsulation and Construct Culture

OPF and Ac-PEG-RGD were fabricated as described previously. Constructs were fabricated at OPF/PEG-DA/PEG-diSH ratios of 60:20:20 (w/w/w) and 60:40:0 (w/w/w) and Ac-PEG-RGD was incorporated at 0.01 g/mL when needed. The polymers were sterilized via exposure to UV light for 3 hours and then dissolved in sterile PBS. The solutions were placed in a 37^{o}C oven for 20 minutes to eliminate air bubbles and then the cell solution was added for a final concentration of 10E6 cells/mL. The sterile photo-initiator was added (0.05% D2959 in 10% NVP) and the solution was placed into Teflon

molds (~30 μL) and polymerized under the UV lamp for 13 minutes. The constructs were placed in 12-well tissue culture plates and 2 mL growth medium was added to each well. The media was changed both one hour and one day after encapsulation, then every 2-3 days thereafter.

Cell Viability Analysis

At timepoints where cell viability was assessed, the constructs (n=3) were placed in 4 mL sterile PBS in the incubator for an hour to rinse out the media. The constructs were incubated in a LIVE/DEAD cell-mediated cytotoxicity solution (0.1% 1mM calcein, 0.05% ethidium homodimer-1; Invitrogen) for 45 minutes in foil, and then rinsed in 2 mL PBS for 1 minute to remove excess dye. Stained constructs were imaged on a LSM 510 Confocal Microscope (Zeiss) for cell viability.

Image Analysis

At each timepoint, five surface and interior images (~500-800 μm below the surface) of each construct were taken and exported to the ImageJ software (NIH) for area and circularity analysis. The images were taken from the center of the constructs and at four points forming a rectangle around the center near the edges of the constructs (Figure 1). The green channel (live cells) of all images were converted to gray scale and thresholded for any particles with brightness levels lower than 30 (out of 255; value was arbitrarily chosen). Particles of a minimum size of 15 pixels were identified and the area (A) and perimeter (P) were calculated based on the pixel size (scale conversion of

images: 512 pixels = 921 μm). The circularity was calculated from the equation $4\pi A/P^2$, thus a perfect circle would have a circularity value of 1.0.

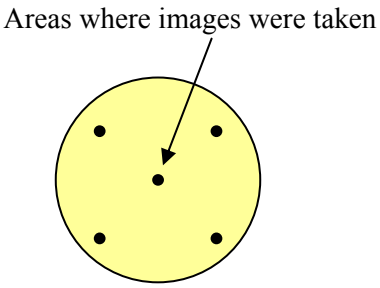

Figure 1. Schematic of the top view of the hydrogels indicating where images were taken for viability and cell area/circularity analysis. Surface and interior images (~500-800 μm below surface) were taken at each of five locations on each hydrogel (indicated by black dots) for use in cell viability, area, and circularity analysis.

DNA Content and Collagen Synthesis

At each timepoint, the constructs (n=4) were rinsed in PBS to remove the media and their wet weights recorded. The hydrogels were placed in individual wells of a 24-well tissue culture plate and ground using pellet grinders. The gel pieces were covered with 500 μL of a 1 mg/mL proteinase K digestion buffer (Tris/EDTA buffer, iodacetamide, pepstatin A, proteinase K) and heated in a 37°C water bath for 30 minutes. The samples were then stored at -20°C until further analysis. Before analysis, the samples were placed in a 60°C waterbath for at least 16 hours to enable proteinase K digestion.

DNA Content

DNA content was assessed using the Quant-iT PicoGreen dsDNA Assay kit (Invitrogen). Briefly, 43 μL of sample, 107 μL of buffer, and 150 μL of PicoGreen

solution were pipetted into a 96-well opaque, flat-bottomed assay plate. The fluorescence was read at exitation: 485 nm and emission: 525 nm and compared to a standard curve from DNA provided in the kit. DNA content was also assessed for cells used for encapsulation to calculate the amount of DNA (pg) per cell. Cells were counted on a hemocytometer on the day of encapsulation and 100,000 cells were pelleted and digested with proteinase K (see above) and assayed using PicoGreen.

Total Collagen Content

Total collagen content was assessed by measuring the amount of hydroxyproline available in the sample. The samples were hydrolyzed in a 1:1 dilution with 12M hydrochloric acid (HCl; Sigma-Aldrich) at 110^{o}C for at least 16 hours. The HCl was then evaporated off under a stream of nitrogen and the hydrolyzate was resuspended in 0.5 mL distilled water (dH_2O). The sample was pipetted (100 µL) in a 96-well clear, UV transparent flat-bottomed assay plate with 50 µL chloramine-T solution (chloramine-T (Sigma-Aldrich), isopropanol, and buffer) and incubated at room temperature for 20 minutes. Then, 50 µL of a solution containing 4-(dimethylamino)benzaldehyde (Sigma-Aldrich), isopropanol, dH_2O, and 70% perchloric acid was pipetted into each well and the plate was put in a 60^{o}C water bath for 30 minutes. After the plate was cooled, the absorbance (570 nm) was read and compared to a *trans*-4-hydroxy-L-proline standard curve (Sigma-Aldrich).

Statistical Analysis

Data from all studies was analyzed using Minitab statistical software (version 15.1.1.0; Minitab, Inc.) for analysis of variance (ANOVA) with Tukey's Multiple Comparison Test ($p \leq 0.05$).

CHAPTER 3

RESULTS

Hydrogel Swelling & Degradation

OPF Synthesis and Characterization

GPC analysis indicated that the OPF synthesized had an average M_n of 13,240 and a polydispersity index (PI) of 5.8, while the corresponding PEG used for macromer synthesis had an average M_n of 6,820 with a PI of 1.5. NMR results for the OPF showed the appearance of peaks at 6.8 ppm (data not shown), indicating the presence of fumarate groups within the molecules[63].

Swelling Characteristics

The effect of OPF incorporation on the swelling characteristics of hydrogels containing PEG-diSH and hydrogels containing no PEG-diSH at 60% initial water content was assessed through the fold swelling after 24 hours (Figure 2). Tri-ratio hydrogel formulations ranged from 40-60% OPF (by weight) and had either PEG-DA alone or a 50:50 ratio of PEG-DA to PEG-diSH to make up the rest of the weight. The amount of OPF incorporated did not significantly change the fold swelling of hydrogels containing PEG-diSH or those containing no PEG-diSH. The thiol containing hydrogels had significantly increased fold swelling over the non-thiol containing gels.

In a second swelling study, the effect of initial water content on the fold swelling of tri-ratio hydrogels was determined (Figure 3). Hydrogels containing OPF/PEG-DA/PEG-diSH ratios of 60:20:20 and 60:40:0 (w/w/w) were fabricated at 60% and 75% initial water percentages to compare their fold swelling. While the difference in initial

water did not significantly change the fold swelling of non PEG-diSH containing hydrogels, it did significantly increase the fold swelling of the hydrogels containing PEG-diSH.

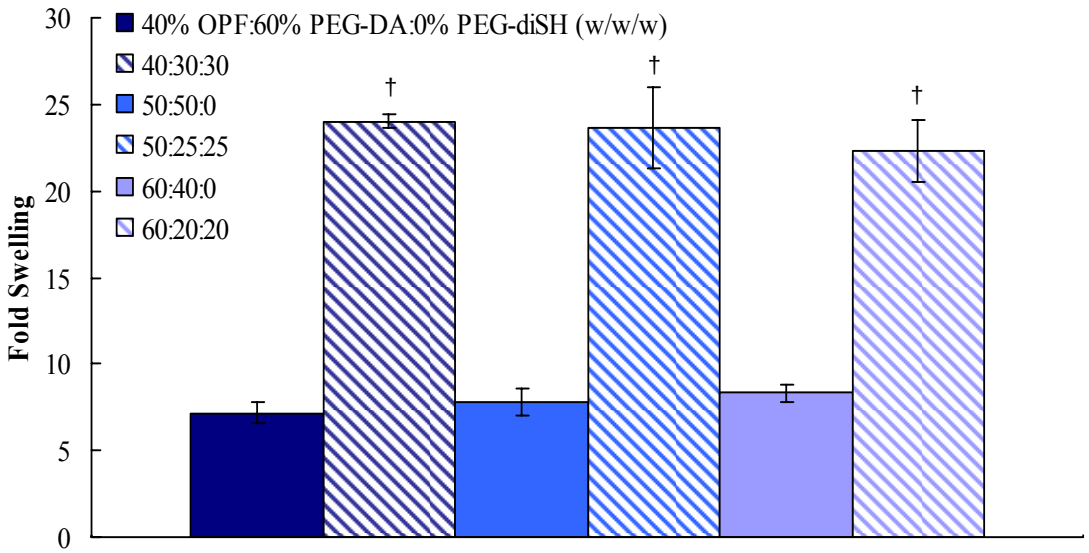

Figure 2. Fold swelling for OPF/PEG-DA/PEG-diSH tri-ratio hydrogels at 60% initial water percentage. Fold swelling calculations of hydrogels containing varying ratios of OPF/PEG-DA/PEG-diSH (w/w/w) after 24 hours swelling in PBS showed that the amount of OPF incorporated did not significantly affect the swelling characteristics of hydrogels containing PEG-diSH (striped) or gels containing no PEG-diSH (solid). († $p \leq 0.05$ compared to non-thiol version of that formulation, $n = 4$)

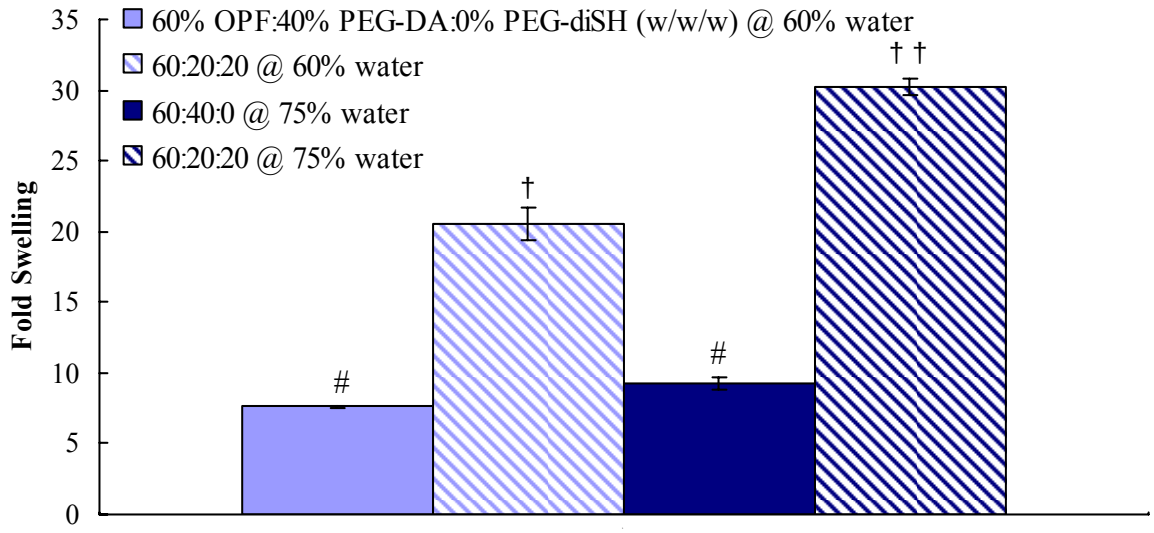

Figure 3. Fold swelling comparisons between OPF/PEG-DA/PEG-diSH tri-ratio hydrogels at 60% and 75% initial water percentages. Fold swelling calculations of tri-ratio hydrogels polymerized with different initial water contents after 24 hours swelling in PBS showed that the initial water content did not significantly change the swelling of hydrogels containing no PEG-diSH (solid bars) while swelling significantly increased in the PEG-diSH samples (striped bars) at the higher initial water percentage. (# indicates significantly lower than both formulations containing PEG-diSH; † indicates significantly greater than both non PEG-diSH formulations; †† indicates significantly greater than all other ratios; $p \leq 0.05$, n = 3)

Degradative Properties

The degradation characteristics (fold swelling and dry weights over time) of PEG-diSH containing hydrogels were compared to non-thiol containing hydrogels (Figures 4 and 5, respectively). The 60:20:20 OPF/PEG-DA/PEG-diSH (w/w/w) formulation had significantly higher swelling characteristics than the other gel types and its swelling also increased over time (Figure 4). These samples were completely degraded by Day 15. While the hydrogel formulation containing 10% PEG-diSH swelled more than the hydrogels containing no PEG-diSH, the fold swelling for both of these gel types remained constant over the timecourse. The dry weight of the 20% thiol gels also significantly decreased by Day 5 while the dry weights of the other gel types remained constant over the timecourse (Figure 5).

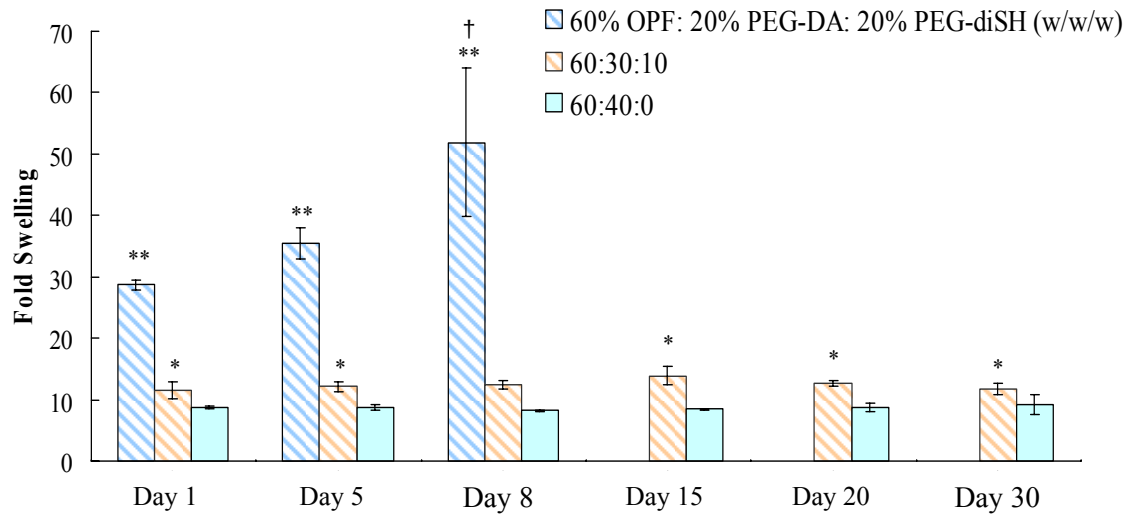

Figure 4. Degradation characteristics of OPF/PEG-DA/PEG-diSH hydrogels and OPF/PEG-DA control gels at 75% initial water percentage. Fold swelling parameters were calculated for gels containing varying amount of PEG-diSH at Days 1, 5, 8, 15, 20, and 30. The formulation incorporating 20% PEG-diSH (by weight) had significantly increased swelling properties over the other gel types, and demonstrated increased fold swelling over time, eventually degrading completely by Day 15. The swelling properties of the formulations containing 10% PEG-diSH and no PEG-diSH remained constant over time. († indicates significantly greater than Days 1 and 5 for that formulation; * indicates significantly greater than the 60:40:0 ratio at that timepoint; ** indicates significantly greater than all other ratios at that timepoint; $p \leq 0.05$, $n = 4$)

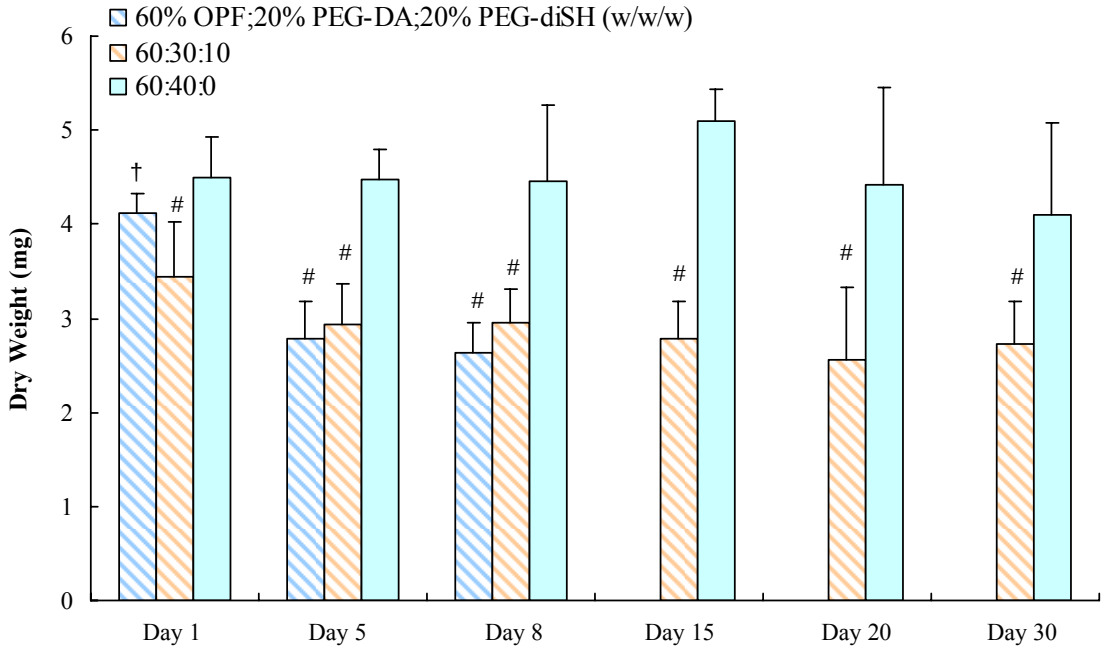

Figure 5. Dry weights of OPF/PEG-DA/PEG-diSH hydrogels and OPF/PEG-DA control gels. Dry weights of the hydrogels were recorded at Days 1, 5, 8, 15, 20, and 30. The formulation incorporating 20% PEG-diSH (by weight) had significantly decreased dry weight by Day 5. The dry weights of the other two formulations remained constant over time. († indicates significantly greater than Days 5 and 8 for that formulation; # indicates significantly less than the 60:40:0 ratio at that timepoint; $p \leq 0.05$, $n = 4$)

Cell Encapsulation in Hydrogel Constructs

Cell Viability Analysis

The effects of initial water concentration and the presence of PEG-diSH on the viability of tendon/ligament fibroblasts were assessed over one week (Figure 6). The constructs containing 60% initial water were non-viable at Day 1 and remained so over one week, regardless of the presence of PEG-diSH. The cells encapsulated at 75% initial water content were viable over one week of culture, both with and without the presence of PEG-diSH.

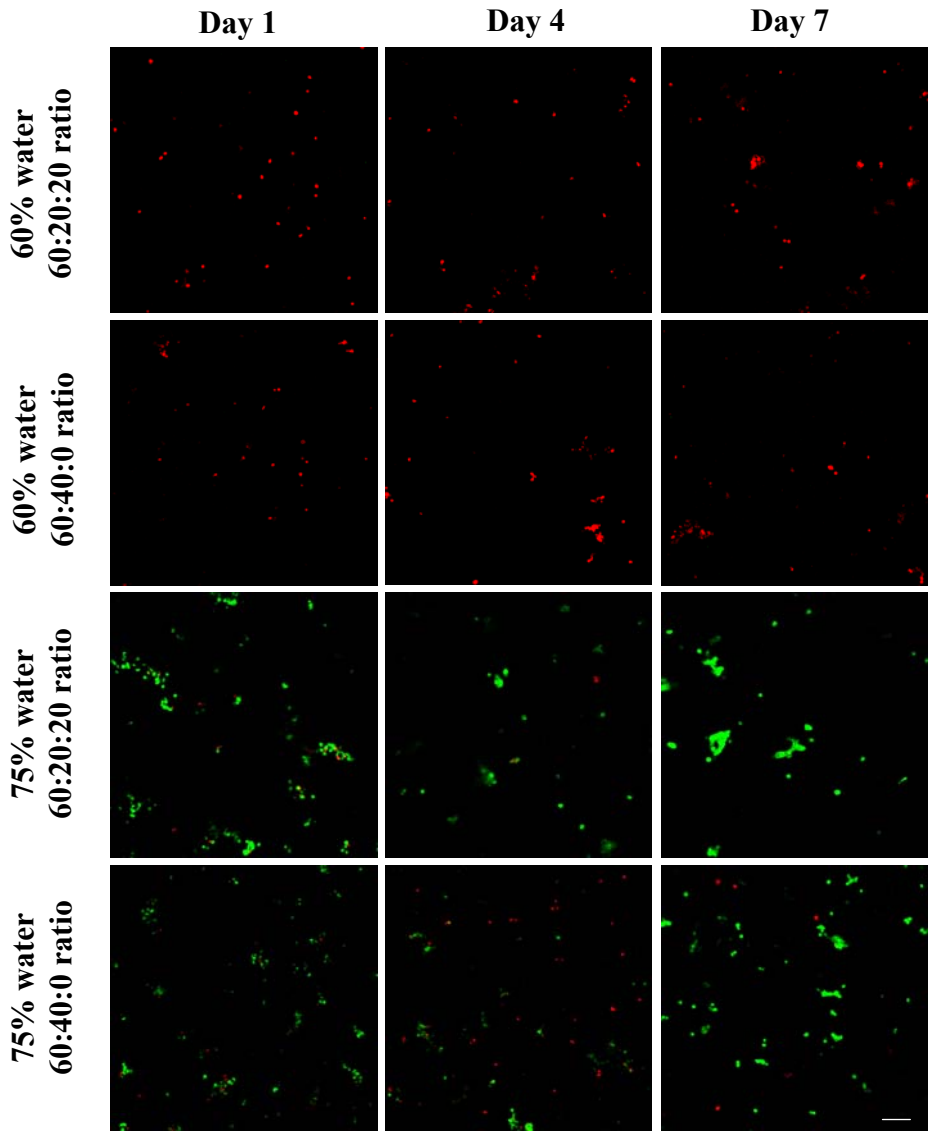

Figure 6. Viability (LIVE/DEAD) analysis of tendon/ligament fibroblasts encapsulated in OPF 10K/PEG-DA/PEG-diSH hydrogels at 60% and 75% initial water percentages. Confocal microscope images of encapsulated cells were taken on Days 1, 4, and 7 of culture. Green dye (calcein AM) indicates live cells and red dye (ethidium homodimer) indicates dead cells. Cells encapsulated in hydrogels containing 60% initial water did not appear to survive the initial polymerization and remained non-viable throughout the culture period, regardless of the amount of PEG-diSH present. In contrast, cells encapsulated in hydrogels containing both PEG-diSH and no PEG-diSH at 75% initial water appeared mainly viable over the timecourse, with only a few dead cells observed in the constructs by Day 7. (Scale bar = 100 μm; n = 2)

The effect of the Arg-Gly-Asp adhesion ligand (RGD) on the viability (Figure 7) and cell morphology (Figure 8) of tendon/ligament fibroblasts encapsulated in hydrogels containing PEG-diSH or no PEG-diSH was investigated over three weeks with timepoints determined by the previous degradation study. The constructs containing

PEG-diSH showed large clumps of live cells, with very little red staining by Day 8. A majority of viable cells was observed over the 20 day timecourse for the non PEG-diSH containing gels regardless of the presence of RGD.

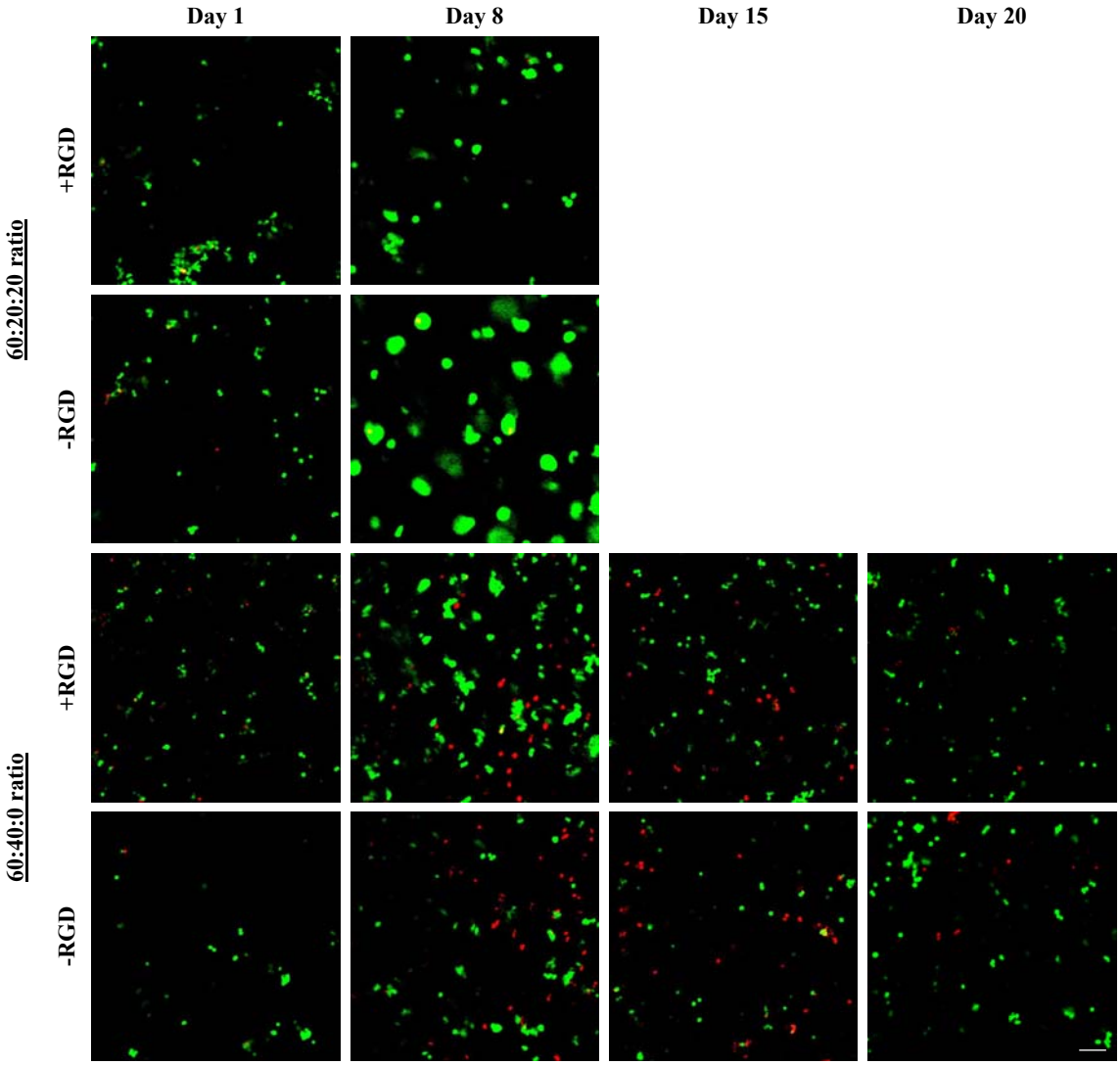

Figure 7. Viability (LIVE/DEAD) of tendon/ligament fibroblasts encapsulated within OPF/PEG-DA/PEG-diSH hydrogels ± RGD adhesion peptide. Confocal microscope images of hydrogels were taken on Days 1, 8, 15 and 20 of culture. Green dye (calcein AM) indicates live cells and red dye (ethidium homodimer) indicates dead cells. By Day 8, the PEG-diSH containing gels showed large clumps of live cells and very little red staining. The non PEG-diSH containing gels showed majority of viable cells over the twenty day timecourse. The gels containing PEG-diSH degraded by Day 15. (Scale bar = 100 μm; n = 3)

The effect of the presence of RGD on cell morphology between the surface and interior of the constructs and between PEG-diSH and non PEG-diSH containing samples

can be seen in Figure 8. At Day 8, there was cell spreading at the surface of the RGD containing samples, regardless of the presence of PEG-diSH. Also at this timepoint, the non-RGD PEG-diSH constructs appeared to have formed larger cell clusters than the non-RGD non PEG-diSH samples (quantified in next section).

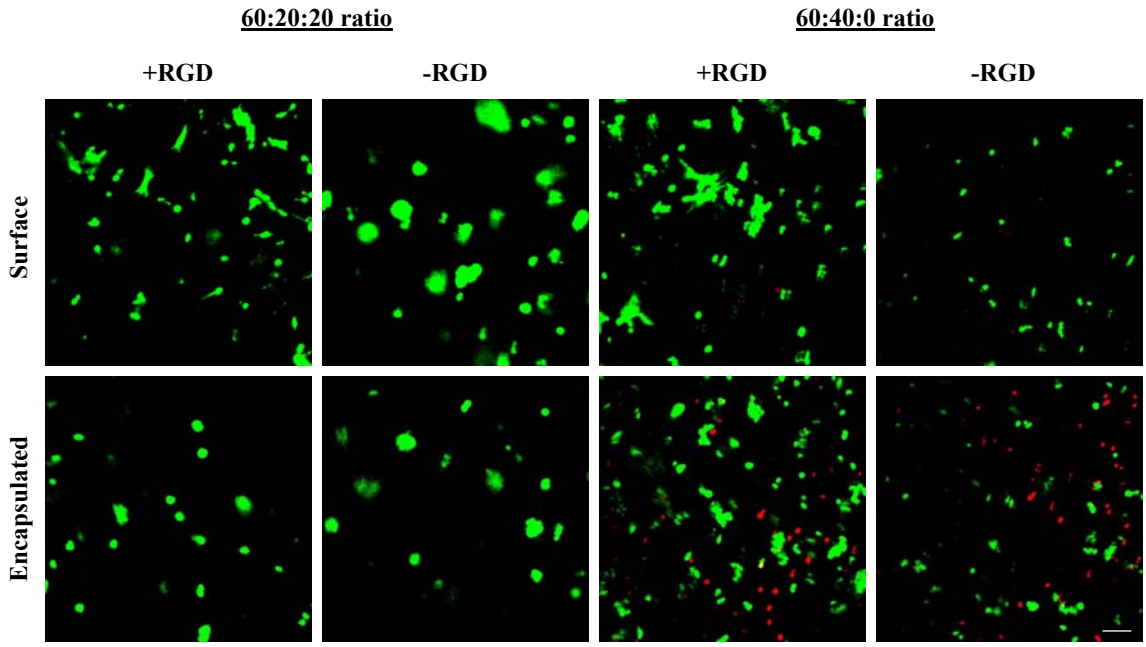

Figure 8. Comparison of morphology between ligament fibroblasts located at the surface and encapsulated within hydrogels ± PEG-diSH and ± RGD. Confocal microscope images of hydrogels were taken on Day 8 of culture. Green dye (calcein AM) indicates live cells and red dye (ethidium homodimer) indicates dead cells. By Day 8, the non-RGD PEG-diSH containing gels appeared to have larger cell clusters than the non-RGD control gels, both on the surface and within the gels. Also at Day 8, cell spreading can be seen on the surface of RGD containing hydrogels, regardless of the presence of PEG-diSH. (Scale bar = 100 μm; n = 3)

Image Analysis

The average area per cell (μm^2) was calculated for surface and interior images of each gel type (Figure 9). In some cases, the average area of a cell cluster was calculated as the imaging software can not distinguish between cell clumps and individual cells. The average cell area at the surface (Figure 9A) of thiol-containing hydrogels with RGD (Thiol + RGD) was significantly larger at Day 1 than that of cells on the thiol-containing

gels without RGD (Thiol – RGD), but the area of cells on the Thiol – RGD samples significantly increased by Day 8, while those on the Thiol + RGD gels did not. Also at Day 8, the cells on the Thiol – RGD gels had significantly greater area than those on the non thiol-containing samples without RGD (DA – RGD). The average area of cells at the surface of non thiol-containing gels with RGD (DA + RGD) significantly decreased by Days 15 and 20. The area of cells encapsulated (Figure 9B) in both thiol-containing formulations (± RGD) and the DA + RGD samples significantly increased by Day 8 with the area of the cells in both thiol-containing formulations larger than those in the non thiol-containing gels. The average area decreased by Days 15 and 20 in the DA + RGD gels.

At Day 1, cells on the surface of the Thiol + RGD gels were significantly larger in area than cells encapsulated within that formulation and both non thiol-containing formulations (± RGD). Also at Day 1, cells on the surface of both DA formulations (± RGD) had significantly larger areas than cells encapsulated within the DA + RGD gels. By Day 8, cells on the surface of Thiol – RGD gels had significantly larger areas than cells encapsulated in DA – RGD hydrogels, and cells within Thiol – RGD gels had larger areas than cells on the surface of DA – RGD gels. There were no significant differences between surface and encapsulated cells at Day 15, but by Day 20, cells on the surface of both DA formulations (± RGD) were significantly larger than cells encapsulated within those gel types.

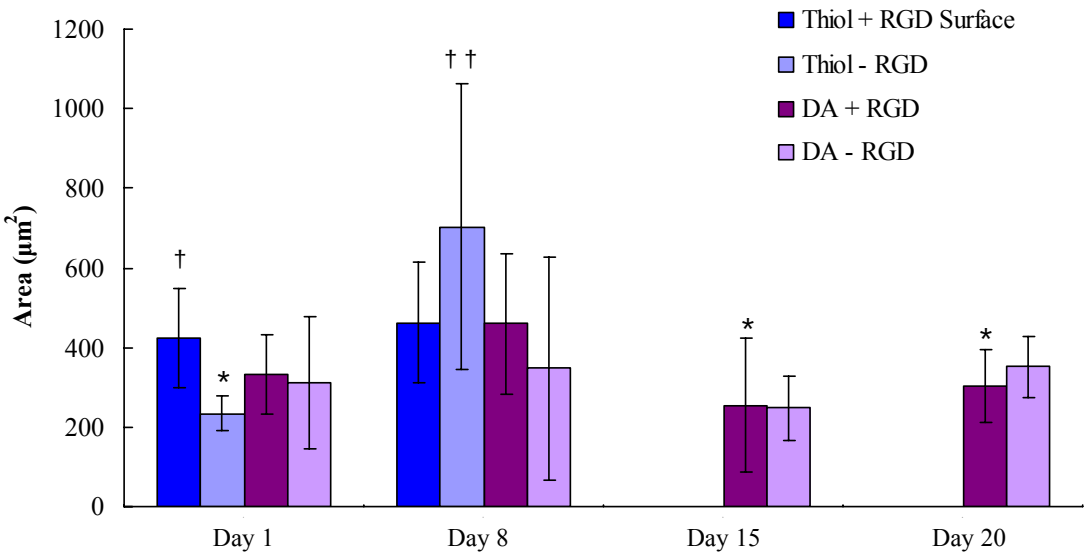

Figure 9A. Cell area analysis of surface images from PEG-diSH (Thiol) and non PEG-diSH (DA) containing hydrogels ± RGD. Five images from the surface of each gel were analyzed using ImageJ software for average particle area (μm^2). Cells on the Thiol gels without RGD (Thiol – RGD) demonstrated significantly larger area at Day 8 versus Day 1. (* indicates significantly smaller than Day 8 for that formulation; † indicates significantly larger than the Thiol – RGD formulation at that timepoint; †† indicates significantly larger than the DA – RGD formulation at that timepoint; $p \leq 0.05$, $n = 3$)

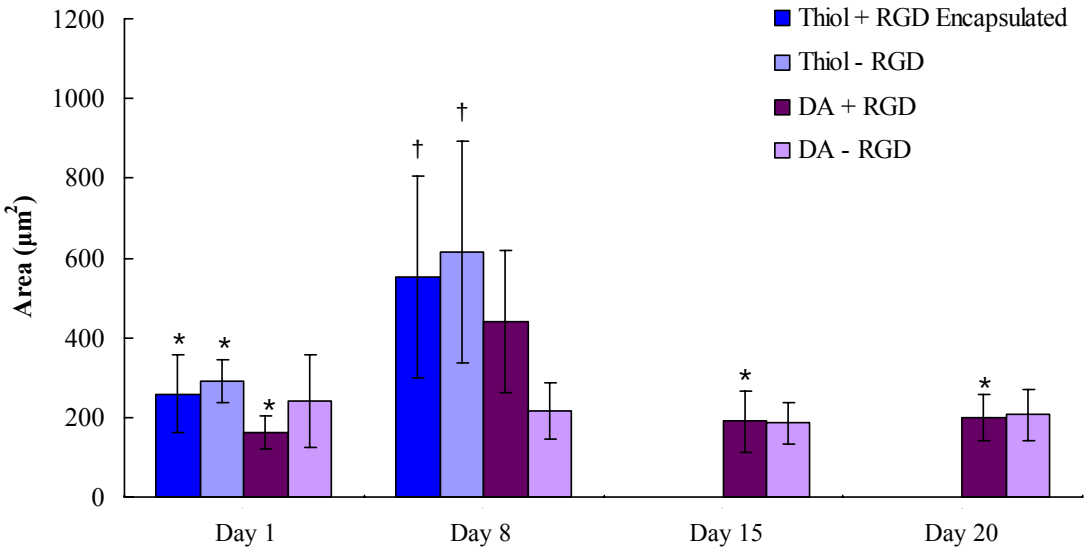

Figure 9B. Cell area analysis of interior images of PEG-diSH (Thiol) and non PEG-diSH (DA) containing hydrogels ± RGD. Five images from within each gel were analyzed using ImageJ software for average particle area (μm^2) of encapsulated cells. By Day 8, cells encapsulated in both Thiol formulations (± RGD) and the DA + RGD formulation were significantly larger in area than on Day 1. Also by Day 8, cells encapsulated in both Thiol formulations (± RGD) were larger in area than the DA-RGD formulation. (* indicates significantly smaller than Day 8 for that formulation; † indicates significantly larger than the DA – RGD formulation at that timepoint; $p \leq 0.05$, $n = 3$)

The average circularity of the cells was analyzed for surface and interior images of each gel type (Figure 10). A circularity value of 1 indicates a round cell while values less than this indicate increasing spreading. At Day 1, cells on the surface (Figure 10A) of Thiol – RGD gels were significantly less spread than all other gel formulations, and by Day 8, cells at the surface of all hydrogel types were significantly more spread than at Day 1. Also at Day 8, cells on gels containing RGD (both Thiol and DA) were more spread than cells on the DA – RGD samples. By Day 15, cells at the surface of the DA + RGD gels were more spread than cells on the surface of the DA – RGD samples. Also by Day 15, cells on the surface of the DA – RGD samples demonstrated decreased spreading compared to Day 8. Cells encapsulated (Figure 10B) in the hydrogels also showed increased spreading by Day 8, with the cells in the Thiol + RGD gels spreading more than cells in both formulations without RGD (Thiol and DA). By Day 15, the cells in the DA + RGD samples had significantly more spreading than cells in the DA – RGD gels. By Day 20, cells encapsulated within the DA + RGD samples had decreased spreading compared to Days 8 and 15.

At Day 1, cells on the surface of the Thiol – RGD samples were significantly less spread than cells encapsulated within Thiol + RGD samples and both DA formulations (± RGD). Also at Day 1, cells encapsulated within Thiol – RGD and DA + RGD samples were less spread than cells on the surface of the DA – RGD samples. By Day 8, cells encapsulated within the Thiol + RGD gels were more spread than cells on the surface of Thiol – RGD and DA – RGD samples. Cells on the surface of DA + RGD and Thiol + RGD gels were more spread than cells encapsulated within DA – RGD gels. Cells encapsulated within DA + RGD gels were more spread than cells on the surface of DA –

RGD gels. At Day 15, cells on the surface of DA + RGD gels were more spread than cells encapsulated within DA – RGD gels and cells encapsulated within DA + RGD gels were more spread than cells on the surface of DA – RGD gels.

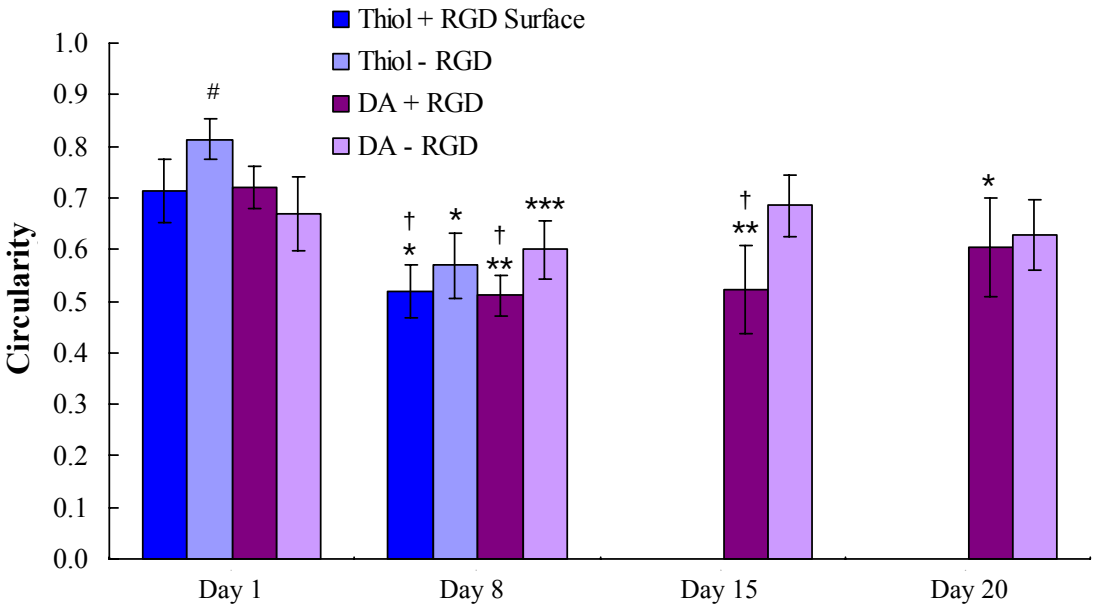

Figure 10A. Cell circularity analysis of surface images of PEG-diSH (Thiol) and non PEG-diSH (DA) containing hydrogels ± RGD. Five images from the surface of each gel were analyzed using ImageJ software for average circularity of cells (a value of 1 indicates a round particle). By Day 8, cells at the surface of all hydrogel types had started to spread, with cells on hydrogels containing RGD spreading more than those on DA – RGD gels. (* indicates significantly more spread than Day 1 for that formulation; ** indicates significantly more spread than Days 1 and 20 for that formulation; *** indicates significantly more spread than Days 1 and 15 for that formulation; # indicates significantly less spread than all other formulations at that timepoint; † indicates significantly more spread than the DA – RGD formulation at that timepoint; $p \leq 0.05$, $n = 3$)

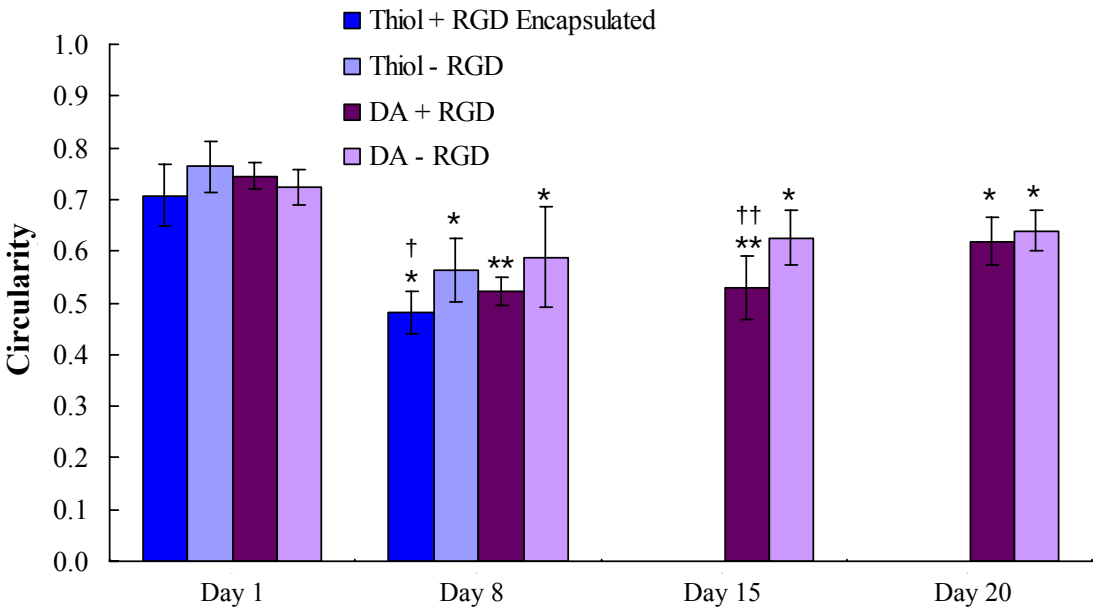

Figure 10B. Cell circularity analysis of encapsulated images of PEG-diSH (Thiol) and non PEG-diSH (DA) containing hydrogels ± RGD. Five images from within each gel were analyzed using ImageJ software for average circularity of cells encapsulated in the hydrogels (a value of 1 indicates a round particle). By Day 8, cells encapsulated in all formulations had spread significantly, with cells in the Thiol + RGD hydrogels spreading more than those in formulations without RGD (both Thiol and DA). (* indicates significantly more spread than Day 1 for that formulation; ** indicates significantly more spread than Days 1 and 20 for that formulation; † indicates significantly more spread than the Thiol – RGD and DA – RGD formulations at that timepoint; †† indicates significantly more spread than the DA – RGD formulation at that timepoint; $p \leq 0.05$, $n = 3$)

DNA Content and Collagen Synthesis

The DNA content of the hydrogels was assessed through the PicoGreen assay at Days 1, 5, 8, 15 and 20 and converted to cell number (Figure 11). At Day 1, the number of cells in the samples was about one third of the original seeding density of the hydrogels (300,000 cells/gel). Although there was no discernable trend between the gel formulations at the earlier timepoints, the number of cells in the samples significantly decreased by Days 15 and 20. PicoGreen performed on acellular gels cultured through Day 8 did not show any discernable DNA content (data not shown). The total collagen content of the samples, as determined by the hydroxyproline assay, was calculated by

subtracting the values of the blank gels at Day 8, resulting in negative values for collagen production (Figure 12).

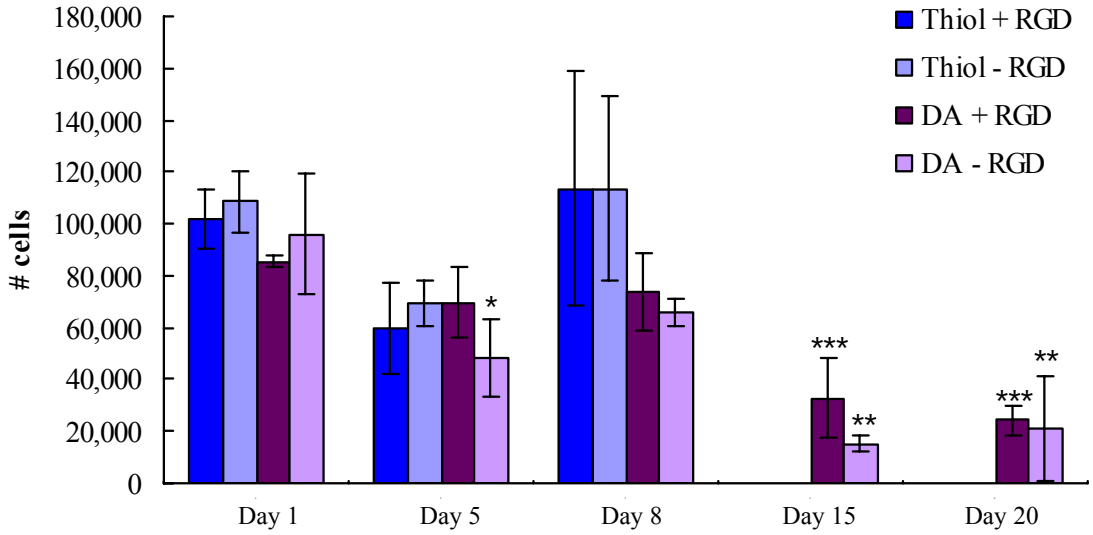

Figure 11. Cell number converted from DNA content for PEG-diSH (Thiol) and non PEG-diSH (DA) containing hydrogels ± RGD. The PicoGreen DNA content assay was performed on hydrogels at Days 1, 5, 8, 15 and 20 of culture and converted to cell number. Although no trend between gel formulations was apparent over the timecourse, by Day 15, the number of cells in the DA ± RGD samples had decreased significantly from Day 1. (* indicates significantly less cells than Day 1 for that formulation; ** indicates significantly less cells than Days 1 and 8 for that formulation; *** indicates significantly less cells than Days 1, 5 and 8 for that formulation; $p \leq 0.05$, $n = 4$)

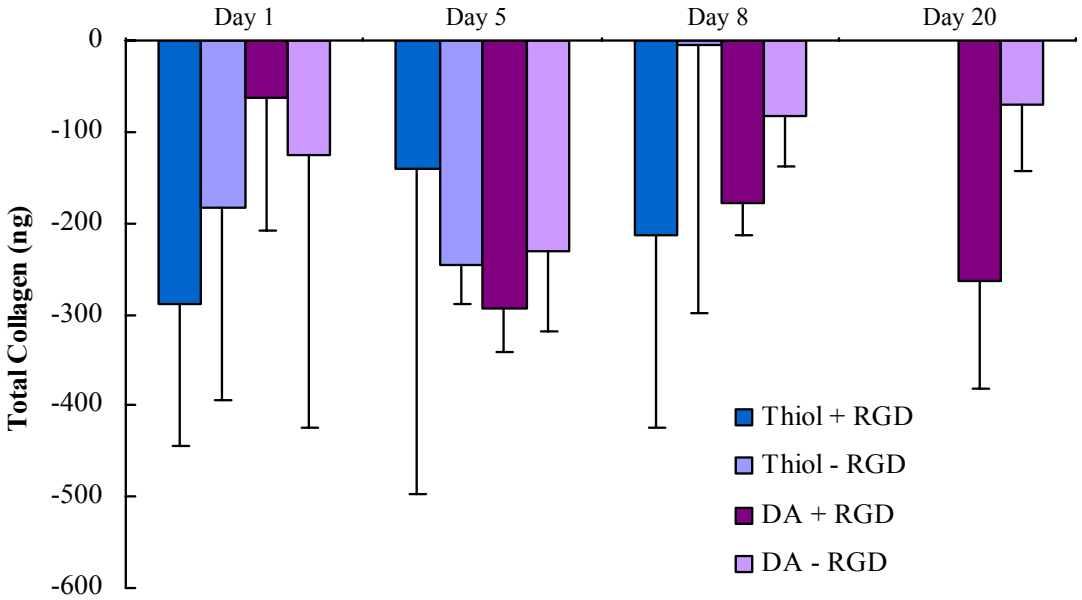

Figure 12. Collagen content for PEG-diSH (Thiol) and non PEG-diSH (DA) containing hydrogels ± RGD. The hydroxyproline total collagen assay was performed on hydrogels at Days 1, 5, 8 and 20 of culture. Acellular gels cultured through Day 8 were also assayed and subtracted as blank values. Although there was no trend at the earlier timepoints, there was a significant difference in collagen production between the DA gels by Day 20. (n = 4)

CHAPTER 4

DISCUSSION

Hydrogel Fabrication

Swelling Characteristics

The first goal of this thesis project was to characterize the swelling and degradative properties of hydrogels containing three components – OPF, PEG-DA, and PEG-diSH. Previous work has shown that hydrogels or bio-functionalized polymers can be made through the Michael-type addition reaction of thiol groups and acrylate end groups[49, 51-58]. This coupling between thiol groups and acrylate end groups can then be combined with a radically-initiated crosslinking reaction, creating a mixed-mode reaction scheme that produces a covalently crosslinked network[49]. The use of this mixed-mode reaction with OPF is advantageous as it adds another degree of freedom to our hydrogel formulations, it allows for the possibility of adding biofunctional groups, such as matrix-metalloproteinase cleavable sequences[49-58], into our hydrogels, and it may increase degradation of the gels[49, 50, 61, 62]. A first step in the use of this polymerization scheme in our laboratory is to ascertain whether mixed-mode polymerization will work in the presence of OPF and better understand how it affects hydrogel properties and cell viability.

In this work, hydrogels were made containing a combination of OPF, PEG-DA and PEG-diSH to examine the effects of both the OPF and the PEG-diSH on the physical properties of the hydrogels. The results of the first swelling study showed that the presence of PEG-diSH in the system significantly increased the fold swelling of the hydrogels. Since the difference in fold swelling between gels containing PEG-diSH and

those not containing PEG-diSH was so large, the effect of the initial water content on the swelling properties of the hydrogels was investigated to determine if the fold swelling changed with an increase in the initial water content. Hydrogels containing OPF/PEG-DA/PEG-diSH ratios of 60:20:20 and 60:40:0 (w/w/w) at 60% and 75% initial water contents were fabricated and swollen for 24 hours. The increase in initial water resulted in increased swelling of the gels containing PEG-diSH, while the water content did not affect the swelling of the non-thiol hydrogels.

Degradative Properties

The degradative properties of hydrogels containing 60% OPF (by weight) and varying amounts of PEG-diSH were determined over 30 days compared to control gels containing no PEG-diSH. The hydrogels containing the largest amount of PEG-diSH (20% by weight) demonstrated greater swelling and earlier degradation times (less than 15 days versus greater than 30 days) than the other gel types. These gels also had significantly decreased dry weights by Day 5, indicating degradation and loss of polymer. The 10% PEG-diSH samples did swell significantly more than the DA only gels, but did not show evidence of degradation over the time period studied, as shown by the constant fold swelling and dry weights over the 30 days. The reason why the hydrogels containing 10% thiol did not degrade, but those containing 20% thiol did can be explained by the kinetics of the mixed-mode reaction that occurs between the thiol and acrylate groups in the system[49, 50]. The ratio of PEG-DA to PEG-diSH affects the reaction chemistry and therefore alters the material properties of the resulting hydrogel. The network structure in degradable thiol-acrylate materials is comprised of thiolpolyacrylate backbone chains that

are connected to each other through degradable cross-links. The distribution of the thiolpolyacrylate backbone chain lengths is controlled through the thiol functionality, the ratio of thiol and acrylate functional groups in the initial monomer mixture, and the amount of acrylate homopolymerization that occurs relative to chain transfer to thiol[49, 50, 64]. Changing the DA:diSH ratio from 30:10 to 20:20 could have altered the reaction chemistry and increased the mesh size enough that it produced a network where fewer links need to be cleaved before the network fell apart. Also, as discussed previously, hydrogels fabricated through the thiol-acrylate mixed-mode reaction scheme degrade hydrolytically through cleavage of ester linkages, and those ester groups located nearer to sulfide bonds may be cleaved faster[49, 50, 61, 62]. Increasing the PEG-diSH in the hydrogels to 30% of the total polymer weight could have decreased the distance between ester and sulfide groups enough to increase the rate of ester hydrolysis so that the network degrades more readily[55, 62].

Cell Encapsulation in Hydrogel Constructs

Cell Viability Analysis

The swelling studies showed a significant difference in fold swelling between hydrogels containing OPF/PEG-DA/PEG-diSH (w/w/w) ratios of 60:20:20 and 60:40:0 at both 60% and 75% initial water concentrations. Therefore, tendon/ligament fibroblasts were encapsulated in these hydrogels at both initial water concentrations to determine the effects of initial water content and the presence of PEG-diSH on the long term viability of the cells. It appeared that cells encapsulated at 60% initial water content did not survive the initial polymerization process and remained non-viable throughout the one

week timecourse, regardless of the presence of PEG-diSH in the hydrogels. The cells encapsulated at 75% initial water had increased viability at Day 1 and throughout the timecourse. Since previous work has shown that PEG-derivatives and OPF cross-linked with PEG-DA are non-cytotoxic to a variety of cell types[33-35, 38, 39], and that the photoinitiator D2959 is non-toxic to cells[46-48], the viability results for cells encapsulated at 60% initial water content indicate that the amount of water initially present in the hydrogels affects the overall viability of the cells. From the study comparing the fold swelling of the hydrogels at both initial water percentages, the extent of swelling after polymerization, which may affect nutrient diffusion within the constructs, does not seem to be a factor in cell survival since the non-thiol gels at both 60% and 75% initial water have similar fold swelling and the cells in the 75% initial water gels survived well. Therefore, it is likely that the cells did not survive the polymerization process with 60% initial water. With so little water available in these hydrogels, the cells could have dehydrated under the UV lamp during polymerization, or could have been affected by the osmolarity of the pre-crosslinked solution. The higher osmolarity of the solution surrounding the cells would have imbalanced the water concentration across the cell membrane and drawn water out of the cells, causing dehydration and cell death during polymerization.

The incorporation of the adhesion ligand RGD has been shown to promote cell attachment within hydrogel constructs[65-67]. Therefore, the effect of RGD incorporation on cell viability and morphology of ligament fibroblasts was then investigated in these hydrogels at 75% initial water content over three weeks. All gel types exhibited a majority of viable cells over the timecourse of the experiment (although the gels

containing PEG-diSH degraded by Day 15), with no marked differences observed between gels containing RGD and those without RGD.

These results differ from a previous study that encapsulated human mesenchymal stem cells (hMSCs) in hydrogels formed from a mixed-mode polymerization of PEG dimethacrylate and multifunctional peptide monomers and found that the presence of RGD (5mM) sustained cellular viability to 75% which was twice the viability seen in non-RGD gels and gels containing the scrambled non-adhesive RDG peptide[66]. The RGD peptide in this case was covalently incorporated into the hydrogels and tethered into the matrix on both the N- and C-termini of the peptide, perhaps allowing for a more stable environment for the cells to attach and spread on the matrix instead of having the peptide tethered on one end and moving freely within the construct. The same group of investigators has also studied the effects of acrylating one end of an RGD peptide and tethering it to the hydrogel network on the viability of encapsulated cells[68, 69]. In these studies, hMSCs[68] and β-cells[69] were encapsulated in PEG-DA incorporating tethered RGD on a PEG spacer arm. After one week, hMSC viability in the hydrogels improved by 60% over non-RGD gels and β-cells had 60% viable cells after ten days compared to 17% in non-RGD control gels. The differences in results could be due to the cell sources used (human MSCs and mouse β-cells versus bovine fibroblasts) as they all have different growth rates and responses to exogenous signals. Also, the hydrogels used in these studies were fabricated from either PEG-dimethacrylate with RGD tethered at two ends[66], or PEG-DA with RGD tethered at one end[68, 69]. The hydrogels used in this thesis contained a mixture of PEG-DA, PEG-diSH, and OPF which could account for the

discrepancies in long term viability between these studies and the previously published work.

Image Analysis

Overall Cell Area

The overall area per cell (μm^2) was quantitatively assessed through ImageJ analysis of surface and interior images of each gel type. In this method, cell clusters would register as larger in area than single, rounded cells. Over time, there was no difference at the surface of the Thiol + RGD samples between Days 1 and 8, although there was a difference in the area of cells encapsulated within the gels. The cells in the interior of the gels were smaller at Day 1 than at Day 8, indicating clumping had occurred due to the larger mesh size of the gel. The mesh size is the physical size of the openings in a 3D crosslinked network and is related to the end-to-end distance of the polymer chains[70]. Previous studies have found that the mesh size of hydrogels is directly correlated with the swelling properties (larger mesh size allows for more swelling to occur)[70-72].

There was a significant difference between Day 1 and Day 8 on the surface and interior of the Thiol – RGD samples. The area of the cells in both locations were smaller in area at Day 1 than at Day 8, which supports the LIVE/DEAD data and indicates cell clumping in these gels as well, despite the lack of RGD available. The mixed-mode reaction scheme of the system consumes multiple acrylate functional groups for each thiol group that reacts, leading to a system with incomplete thiol conversion[73]. During the reaction, conversion of the thiol monomer is high while the total thiol functional

group conversion is lower, leaving a high thiol concentration that is tethered to the network[73]. Therefore, the cell clumping could also be affected by the free thiol groups in the system that could be interacting with proteins in the media or directly with receptors on the cell surface and inducing signaling responses within the cells.

The cells at the surface of the DA + RGD samples had larger total area at Day 8 than at Days 15 and 20 which could be a result of the fact that the cells at the surface were confluent layers by Day 15 and were probably washed off through during the staining process. The cells encapsulated in DA + RGD gels demonstrated greater area at Day 8 than at Days 1, 15 and 20 which could be an artifact of the reduced cell numbers seen at the later timepoints (discussed below). Lower cell numbers would decrease any cell clumping that was seen at Day 8 and produce smaller area per cell values. There was no significant difference in cell area over time in either the surface or interior images for the DA – RGD formulation. This may be due to the fact that RGD was not present so the cells could not attach and spread and the mesh size was too small (as indicated by the lower fold swelling for this gel type) to allow for cell clumping.

At Day 1, cells at the surface of Thiol + RGD hydrogels had significantly larger area than cells at the surface of Thiol – RGD gels or cells encapsulated within Thiol + RGD gels and both DA gels (± RGD). This is probably due to the presence of RGD at the surface of the Thiol gels allowing for cells to adhere and start spreading by Day 1 without restrictions from the network mesh. Cells at the surface of both DA gels (± RGD) were significantly larger in area than cells encapsulated within DA + RGD gels. Cells encapsulated within the DA gels would not have room to adhere and clump together

due to the smaller mesh size, so cells at the surface of these gels (± RGD) would be more clumped at Day 1.

By Day 8, the cells at the surface of and encapsulated within the DA – RGD samples demonstrated significantly less area than cells in the Thiol – RGD gels (surface and encapsulated). Cells encapsulated within Thiol + RGD gels were significantly larger in area than cells encapsulated within DA – RGD gels. This supports the idea that the mesh size of the Thiol gels is larger and allows for more spreading and clumping of the cells in those gels. The cells encapsulated in the PEG-DA only gels did not seem to be affected by the presence of RGD, as no difference in area was seen inside the gels by Day 20. Cells at the surface of DA gels (± RGD) demonstrated larger area than cells encapsulated within those gels. This may be due to the mesh size of the hydrogels, as the cells do not have much room to attach and cluster/proliferate inside these gels.

Cell Circularity

The overall circularity of the cells was quantitatively assessed through ImageJ analysis of surface and interior images of each gel type. A circularity value of 1 indicates a perfectly round cell, while a value of 0 indicates a perfectly straight (spread) cell. Over time, cells at the surface of and encapsulated within both Thiol gels (± RGD) were significantly more spread at Day 8 than Day 1. This makes sense for the +RGD samples since both the presence of RGD and the large mesh size allow for cell adhesion and spreading both at the surface and within the matrix. However, it was not expected that the cells in the –RGD gels would spread significantly by Day 8, regardless of the presence of PEG-diSH, since no RGD was present. This might be an artifact of the

image processing technique since even though the mesh size in these gels was large enough to allow for cell spreading, the absence of RGD would inhibit this from happening.

Cells at the surface of and encapsulated in the DA gels (± RGD) were more spread at Days 8, 15, and 20 than Day 1 with the exception of the cells at the surface of the DA – RGD formulation, which were only more spread at Day 8 compared to Day 1. Cells at both locations in the DA + RGD gels were also less spread at Day 20 compared to Days 8 and 15, while cells at the surface of DA – RGD gels were less spread at Day 15 compared to Day 8. The cells on the surface of the DA + RGD were very confluent and probably washed off during the staining procedure, and therefore were not captured in the confocal images at Day 20. It was interesting to find that cells in non-RGD gels were more spread at Day 8 than other timepoints, which was not expected since the mesh size in DA gels does not allow for much cell spreading and RGD was not present. As discussed previously, this might be a result from the image processing, since the circularity values of these gels are not much different from Day 1 values and are just barely significantly different.

At Day 1, cells at the surface of Thiol – RGD gels were significantly less spread than cells at the surface of and encapsulated within Thiol + RGD gels and DA ± RGD gels. This was probably due to the large mesh size of the network and the absence of RGD, which allowed for the start of cell clumping by Day 1. Cells at the surface of DA – RGD gels were significantly more spread than cells encapsulated within Thiol – RGD gels and DA + RGD gels. It is interesting that there was a difference in spreading between cells at the surface of DA – RGD over encapsulated cells in the other gel types

at Day 1 since no RGD was present and one day is a relatively short time for cells to adhere and spread significantly. The difference could be due to the way the calculations were made for circularity in that the cells may have been slightly less round after Day 1 that resulted in a statistical difference, even though the values between the surface DA – RGD cells and the other encapsulated cells are very similar.

By Day 8, cells on the surface of hydrogels containing RGD (± PEG-diSH) were more spread than cells on the surface of or encapsulated within DA – RGD gels, indicating that the cells were responding to the presence of the adhesion ligand at the surface, where they had room to attach and grow. Cells encapsulated within Thiol + RGD gels were more spread at Day 8 than cells in both non-RGD formulations, indicating that RGD and possibly some combination of mesh size and free thiols within the system (as discussed previously) allowed for some cell spreading on the interior of the gels by this timepoint. Cells encapsulated within DA + RGD hydrogels were significantly more spread than those on the surface of DA – RGD samples at Day 8, perhaps an artifact of the image processing since the mesh size would have inhibited spreading of the cells inside the gels. By Day 15, cells on the surface of and encapsulated within the DA + RGD samples were significantly more spread than cells on the surface of and within DA – RGD gels indicating RGD significantly increases spreading.

DNA Content and Collagen Synthesis

DNA content was assessed using the PicoGreen assay and converted to cell number per sample. At Day 1, there were approximately 100,000 cells per sample, which was about two-thirds less than the seeding density of the hydrogels. This could be a

result of losing a fraction of the cells during the media change that occurred an hour after polymerization. At that point, any cells that were not encapsulated within the mesh of the gel would be removed. Additionally, the low numbers could be due to the gel grinding and digestion techniques. The gels may not have been homogenized sufficiently to release all of the cells so they could be digested by the proteinase K solution. Regardless, the cell numbers in the non-thiol gels severely dropped by Days 15 and 20, indicating a loss of cells over the timecourse. This phenomenon of cell loss after two weeks has been seen in other cell types encapsulated in OPF/PEG-DA gels[74]. In both studies, the remaining cells at the later timepoints appeared viable, but the loss in overall cell number indicates cell death and loss from the construct over the culture period.

The presence of PEG-diSH did not seem to affect overall cell number, although a trend is hard to discern since the gels degraded by Day 15. From the viability images, it seems that the presence of PEG-diSH did not necessarily affect overall cell number, but rather cell clumping. This clumping may have occurred due to cell migration or proliferation, but the DNA analysis supports the idea that the cell clumping was a result of cell migration through the matrix and not proliferation. As stated previously, proliferation may have occurred, but was not distinguishable by the assay due to the loss of DNA. The cell clumping may have continued and possibly led to proliferation had the gels not degraded

The presence of RGD did not affect the cell numbers in the hydrogels. It was expected that samples containing RGD would have higher cell numbers over the timecourse due to the cells' ability to attach to the synthetic matrix, produce their own matrix and perhaps proliferate over three weeks. The results, however, are consistent

with previous work from our lab that showed that the presence of RGD did not affect the overall cell numbers of bovine mesenchymal stem cells (bMSCs) encapsulated in OPF/PEG-DA gels[74]. As discussed previously, these results contradict previous studies that found that RGD significantly increased viability/cell number of encapsulated hMSCs and β-cells in PEG-DA hydrogels[66, 68, 69]. Possible reasons for the discrepancy could be due to the difference cell sources used, the polymers used in the hydrogels, or the method of RGD incorporation.

The total collagen content was determined through the hydroxyproline assay. All collagen content values were negative, due to the subtraction of the values from the blank gels, suggesting there was no discernable collagen production over the 20 day culture period. It was expected that a production of collagen would have been seen at later timepoints as the cells would have had time to start producing their own matrix and a larger amount of collagen would have been produced in the PEG-diSH gels due to their increased degradability. This was shown in previous work that investigated the role of hydrogel degradability on the production of extra-cellular matrix molecules by encapsulated chondrocytes after 6 weeks[75]. Hydrogels containing 85% degradable crosslinks had significantly higher collagen production than hydrogels containing only 50% degradable crosslinks. Also, collagen II was located throughout the neotissue formed from 85% degradable gels after 6 weeks whereas collagen II was only located pericellulary in the 50% degradable gels[75]. Perhaps increased collagen production may have been seen in the PEG-diSH gels had they not degraded after two weeks.

CHAPTER 5

CONCLUSION

In conclusion, the mixed-mode reaction scheme used in these studies significantly changes the swelling and degradative properties of OPF/PEG-DA hydrogels and is cytocompatible as seen through the viability studies. Degradation in this system is achieved hydrolytically at physiological pH through cleavage of ester linkages[49, 50, 61, 62]. The ratio of PEG-DA to PEG-diSH affects the reaction chemistry and therefore alters the material properties of the resulting hydrogel. Changing the DA:diSH ratio from 30:10 to 20:20 could have altered the reaction chemistry and increased the mesh size enough that it produced a network where fewer links need to be cleaved before the network fell apart. Increasing the PEG-diSH in the hydrogels to 20% of the total polymer weight could have decreased the distance between ester and sulfide groups enough to increase the rate of ester hydrolysis so that the network degrades more readily[55, 62].

The hydrogels containing PEG-diSH promote cell viability and cell clustering, probably due to the larger mesh size (as seen through the increased fold swelling) and possibly due to the presence of free thiol functional groups present in the network from the mixed-mode reaction. The reaction scheme combines a Michael-type conjugation reaction with a radically initiated polymerization reaction that consumes multiple acrylate functional groups for each thiol group that reacts, leading to a system with incomplete thiol conversion[73]. The un-reacted thiol groups could interact with proteins in the media or directly with receptors on the cell surface and influence cell signaling processes that promote clustering in these gels. The increase in cell clustering is supported by an increase in area per cell (or cluster) by Day 8. However, an increase in cell number was

not found in these gels up to eight days, suggesting that cell migration and not proliferation is responsible for the appearance of clusters. Additionally, increased spreading in response to RGD was observed in gels containing PEG-diSH; no spreading was seen in the DA only gels (± RGD), possibly because the mesh size is too small to allow clustering or spreading within the matrix.

The OPF-based mixed-mode scheme used in this study increases the swelling of the hydrogels, is cytocompatible and allows for cell clustering. This system has potential for use in situations where hydrogels are appropriate for tissue engineering (tendon/ligament and other soft tissue regeneration). This system can be used to form pre-fabricated hydrogels or used as an injectable cell carrier for tissue regeneration applications. The ratio of PEG-DA to thiol monomer used in the system will need to be tailored more for future cell encapsulation studies to keep the gels from degrading after one week.

This system would be useful in repair of partial tears/central defects in ligaments where hydrogels are being studied extensively. The ACL, for example, fails to heal after injury which can lead to premature osteoarthritis and disability[24]. Hydrogels being investigated for partial tear repair have been mainly made out of collagen to promote increased recruitment of growth factors associated with healing[23, 24, 32]. The system presented in this thesis would work well in this application, due to the swelling and degradative properties and the biocompatibility. For example, encapsulated cells in this hydrogel system can be injected to fit into the tear site and the cells can aid in the repair process of the injured tissue. In addition, this system will be useful for incorporating proteolytically degradable sequences (matrix-metalloproteinase-cleavable, for example)

into the hydrogels by adding cysteine amino acid residues on each end of the peptide. This can aid in the repair of ligament tissue by adding controlled degradation to hydrogels to allow for cell migration and proliferation within the matrix.

Results from this work suggest that the presence of PEG-diSH could allow cell-cell contact within the clusters which could be useful in systems where direct contact promotes tissue formation or cell differentiation. Cell-cell contact has been investigated in musculoskeletal tissue engineering where reciprocal signaling between the tendon mesenchyme and muscle endpoints has been shown to play an important role during development of the myotendinous junction[76-78]. Cell clustering has been used in micromass culture for differentiation of mesenchymal stem cells into chondrocytes[79-81].

REFERENCES

1. Langer RS, Vacanti JP. Tissue engineering: the challenges ahead. *Scientific American.* 1999;280(4):86-89.

2. Vacanti CA. The history of tissue engineering. *Journal of cellular and molecular medicine.* 2006;10(3):569-576.

3. Vacanti JP, Langer R. Tissue engineering: the design and fabrication of living replacement devices for surgical reconstruction and transplantation. *Lancet.* 1999;354 Suppl 1:SI32-34.

4. Hoffman AS. Hydrogels for biomedical applications. *Advanced drug delivery reviews.* 2002;54(1):3-12.

5. Baroli B. Hydrogels for tissue engineering and delivery of tissue-inducing substances. *Journal of pharmaceutical sciences.* 2007;96(9):2197-2223.

6. Jeong B, Kim SW, Bae YH. Thermosensitive sol-gel reversible hydrogels. *Advanced drug delivery reviews.* 2002;54(1):37-51.

7. Qiu Y, Park K. Environment-sensitive hydrogels for drug delivery. *Advanced drug delivery reviews.* 2001;53(3):321-339.

8. American Academy of Orthopedic Surgeons website. www.aaos.org. January 2007.

9. Johnson RJ. The anterior cruciate: a dilemma in sports medicine. *Int J Sports Med.* 1982;3(2):71-79.

10. Friedman MJ, Sherman OH, Fox JM, Del Pizzo W, Snyder SJ, Ferkel RJ. Autogeneic anterior cruciate ligament (ACL) anterior reconstruction of the knee. A review. *Clin Orthop Relat Res.* 1985(196):9-14.

11. Lu HH, Jiang J. Interface tissue engineering and the formulation of multiple-tissue systems. *Adv Biochem Eng Biotechnol.* 2006;102:91-111.

12. Jackson DW, Grood ES, Arnoczky SP, Butler DL, Simon TM. Cruciate reconstruction using freeze dried anterior cruciate ligament allograft and a ligament augmentation device (LAD). An experimental study in a goat model. *Am J Sports Med.* 1987;15(6):528-538.

13. Jackson DW, Grood ES, Goldstein JD, Rosen MA, Kurzweil PR, Cummings JF, Simon TM. A comparison of patellar tendon autograft and allograft used for anterior cruciate ligament reconstruction in the goat model. *Am J Sports Med.* 1993;21(2):176-185.

14. Petrigliano FA, McAllister DR, Wu BM. Tissue engineering for anterior cruciate ligament reconstruction: a review of current strategies. *Arthroscopy.* 2006;22(4):441-451.

15. Bellincampi LD, Closkey RF, Prasad R, Zawadsky JP, Dunn MG. Viability of fibroblast-seeded ligament analogs after autogenous implantation. *J Orthop Res.* 1998;16(4):414-420.

16. Noth U, Schupp K, Heymer A, Kall S, Jakob F, Schutze N, Baumann B, Barthel T, Eulert J, Hendrich C. Anterior cruciate ligament constructs fabricated from human mesenchymal stem cells in a collagen type I hydrogel. *Cytotherapy.* 2005;7(5):447-455.

17. Altman GH, Horan RL, Lu HH, Moreau J, Martin I, Richmond JC, Kaplan DL. Silk matrix for tissue engineered anterior cruciate ligaments. *Biomaterials.* 2002;23(20):4131-4141.

18. Altman GH, Lu HH, Horan RL, Calabro T, Ryder D, Kaplan DL, Stark P, Martin I, Richmond JC, Vunjak-Novakovic G. Advanced bioreactor with controlled application of multi-dimensional strain for tissue engineering. *J Biomech Eng.* 2002;124(6):742-749.

19. Dunn MG, Liesch JB, Tiku ML, Zawadsky JP. Development of fibroblast-seeded ligament analogs for ACL reconstruction. *J Biomed Mater Res.* 1995;29(11):1363-1371.

20. Lin VS, Lee MC, O'Neal S, McKean J, Sung KL. Ligament tissue engineering using synthetic biodegradable fiber scaffolds. *Tissue engineering.* 1999;5(5):443-452.

21. Cristino S, Grassi F, Toneguzzi S, Piacentini A, Grigolo B, Santi S, Riccio M, Tognana E, Facchini A, Lisignoli G. Analysis of mesenchymal stem cells grown on a three-dimensional HYAFF 11-based prototype ligament scaffold. *Journal of biomedical materials research.* 2005;73(3):275-283.

22. Majima T, Funakosi T, Iwasaki N, Yamane ST, Harada K, Nonaka S, Minami A, Nishimura S. Alginate and chitosan polyion complex hybrid fibers for scaffolds in ligament and tendon tissue engineering. *J Orthop Sci.* 2005;10(3):302-307.

23. Murray MM, Spindler KP, Abreu E, Muller JA, Nedder A, Kelly M, Frino J, Zurakowski D, Valenza M, Snyder BD, Connolly SA. Collagen-platelet rich plasma hydrogel enhances primary repair of the porcine anterior cruciate ligament. *J Orthop Res.* 2007;25(1):81-91.

24. Murray MM, Spindler KP, Ballard P, Welch TP, Zurakowski D, Nanney LB. Enhanced histologic repair in a central wound in the anterior cruciate ligament with a collagen-platelet-rich plasma scaffold. *J Orthop Res.* 2007;25(8):1007-1017.

25. Frank C, Amiel D, Akeson WH. Healing of the medial collateral ligament of the knee. A morphological and biochemical assessment in rabbits. *Acta orthopaedica Scandinavica.* 1983;54(6):917-923.

26. Frank C, Schachar N, Dittrich D. Natural history of healing in the repaired medial collateral ligament. *J Orthop Res.* 1983;1(2):179-188.

27. Spindler KP, Dawson JM, Stahlman GC, Davidson JM, Nanney LB. Collagen expression and biomechanical response to human recombinant transforming growth factor beta (rhTGF-beta2) in the healing rabbit MCL. *J Orthop Res.* 2002;20(2):318-324.

28. Woo SL, Vogrin TM, Abramowitch SD. Healing and repair of ligament injuries in the knee. *The Journal of the American Academy of Orthopaedic Surgeons.* 2000;8(6):364-372.

29. McAndrews PT, Arnoczky SP. Meniscal repair enhancement techniques. *Clinics in sports medicine.* 1996;15(3):499-510.

30. Arnoczky SP, Warren RF, Spivak JM. Meniscal repair using an exogenous fibrin clot. An experimental study in dogs. *The Journal of bone and joint surgery.* 1988;70(8):1209-1217.

31. Wright RW, Parikh M, Allen T, Brodt MD, Silva MJ, Botney MD. Effect of hemorrhage on medial collateral ligament healing in a mouse model. *The American journal of sports medicine.* 2003;31(5):660-666.

32. Murray MM, Spindler KP, Devin C, Snyder BS, Muller J, Takahashi M, Ballard P, Nanney LB, Zurakowski D. Use of a collagen-platelet rich plasma scaffold to stimulate healing of a central defect in the canine ACL. *J Orthop Res.* 2006;24(4):820-830.

33. Benoit DS, Anseth KS. The effect on osteoblast function of colocalized RGD and PHSRN epitopes on PEG surfaces. *Biomaterials.* 2005;26(25):5209-5220.

34. Nuttelman CR, Benoit DS, Tripodi MC, Anseth KS. The effect of ethylene glycol methacrylate phosphate in PEG hydrogels on mineralization and viability of encapsulated hMSCs. *Biomaterials.* 2006;27(8):1377-1386.

35. Nuttelman CR, Tripodi MC, Anseth KS. In vitro osteogenic differentiation of human mesenchymal stem cells photoencapsulated in PEG hydrogels. *Journal of biomedical materials research.* 2004;68(4):773-782.

36. Jo S, Shin H, Mikos AG. Modification of oligo(poly(ethylene glycol) fumarate) macromer with a GRGD peptide for the preparation of functionalized polymer networks. *Biomacromolecules.* 2001;2(1):255-261.

37. Shin H, Quinten Ruhe P, Mikos AG, Jansen JA. In vivo bone and soft tissue response to injectable, biodegradable oligo(poly(ethylene glycol) fumarate) hydrogels. *Biomaterials.* 2003;24(19):3201-3211.

38. Shin H, Temenoff JS, Mikos AG. In vitro cytotoxicity of unsaturated oligo[poly(ethylene glycol) fumarate] macromers and their cross-linked hydrogels. *Biomacromolecules.* 2003;4(3):552-560.

39. Temenoff JS, Shin H, Conway DE, Engel PS, Mikos AG. In vitro cytotoxicity of redox radical initiators for cross-linking of oligo(poly(ethylene glycol) fumarate) macromers. *Biomacromolecules.* 2003;4(6):1605-1613.

40. Shin H, Jo S, Mikos AG. Modulation of marrow stromal osteoblast adhesion on biomimetic oligo[poly(ethylene glycol) fumarate] hydrogels modified with Arg-Gly-Asp peptides and a poly(ethyleneglycol) spacer. *J Biomed Mater Res.* 2002;61(2):169-179.

41. Temenoff JS, Athanasiou KA, LeBaron RG, Mikos AG. Effect of poly(ethylene glycol) molecular weight on tensile and swelling properties of oligo(poly(ethylene glycol) fumarate) hydrogels for cartilage tissue engineering. *J Biomed Mater Res.* 2002;59(3):429-437.

42. Hwang NS, Varghese S, Zhang Z, Elisseeff J. Chondrogenic differentiation of human embryonic stem cell-derived cells in arginine-glycine-aspartate-modified hydrogels. *Tissue engineering.* 2006;12(9):2695-2706.

43. Sebra RP, Reddy SK, Masters KS, Bowman CN, Anseth KS. Controlled polymerization chemistry to graft architectures that influence cell-material interactions. *Acta biomaterialia.* 2007;3(2):151-161.

44. Weber LM, He J, Bradley B, Haskins K, Anseth KS. PEG-based hydrogels as an in vitro encapsulation platform for testing controlled beta-cell microenvironments. *Acta biomaterialia.* 2006;2(1):1-8.

45. Williams CG, Malik AN, Kim TK, Manson PN, Elisseeff JH. Variable cytocompatibility of six cell lines with photoinitiators used for polymerizing hydrogels and cell encapsulation. *Biomaterials.* 2005;26(11):1211-1218.

46. Bryant SJ, Nuttelman CR, Anseth KS. Cytocompatibility of UV and visible light photoinitiating systems on cultured NIH/3T3 fibroblasts in vitro. *Journal of biomaterials science.* 2000;11(5):439-457.

47. Bryant SJ, Anseth KS. Hydrogel properties influence ECM production by chondrocytes photoencapsulated in poly(ethylene glycol) hydrogels. *J Biomed Mater Res.* 2002;59(1):63-72.

48. Burdick JA, Anseth KS. Photoencapsulation of osteoblasts in injectable RGD-modified PEG hydrogels for bone tissue engineering. *Biomaterials.* 2002;23(22):4315-4323.

49. Elbert DL, Hubbell JA. Conjugate addition reactions combined with free-radical cross-linking for the design of materials for tissue engineering. *Biomacromolecules.* 2001;2(2):430-441.

50. Elbert DL, Pratt AB, Lutolf MP, Halstenberg S, Hubbell JA. Protein delivery from materials formed by self-selective conjugate addition reactions. *J Control Release.* 2001;76(1-2):11-25.

51. Heggli M, Tirelli N, Zisch A, Hubbell JA. Michael-type addition as a tool for surface functionalization. *Bioconjugate chemistry.* 2003;14(5):967-973.

52. Hiemstra C, Aa LJ, Zhong Z, Dijkstra PJ, Feijen J. Rapidly in situ-forming degradable hydrogels from dextran thiols through Michael addition. *Biomacromolecules.* 2007;8(5):1548-1556.

53. Lutolf MP, Tirelli N, Cerritelli S, Cavalli L, Hubbell JA. Systematic modulation of Michael-type reactivity of thiols through the use of charged amino acids. *Bioconjugate chemistry.* 2001;12(6):1051-1056.

54. Qiu B, Stefanos S, Ma J, Lalloo A, Perry BA, Leibowitz MJ, Sinko PJ, Stein S. A hydrogel prepared by in situ cross-linking of a thiol-containing poly(ethylene glycol)-based copolymer: a new biomaterial for protein drug delivery. *Biomaterials.* 2003;24(1):11-18.

55. Rydholm AE, Anseth KS, Bowman CN. Effects of neighboring sulfides and pH on ester hydrolysis in thiol-acrylate photopolymers. *Acta biomaterialia.* 2007;3(4):449-455.

56. Rydholm AE, Bowman CN, Anseth KS. Degradable thiol-acrylate photopolymers: polymerization and degradation behavior of an in situ forming biomaterial. *Biomaterials.* 2005;26(22):4495-4506.

57. Rydholm AE, Reddy SK, Anseth KS, Bowman CN. Controlling network structure in degradable thiol-acrylate biomaterials to tune mass loss behavior. *Biomacromolecules.* 2006;7(10):2827-2836.

58. Vanderhooft JL, Mann BK, Prestwich GD. Synthesis and characterization of novel thiol-reactive poly(ethylene glycol) cross-linkers for extracellular-matrix-mimetic biomaterials. *Biomacromolecules.* 2007;8(9):2883-2889.

59. Lutolf MP, Lauer-Fields JL, Schmoekel HG, Metters AT, Weber FE, Fields GB, Hubbell JA. Synthetic matrix metalloproteinase-sensitive hydrogels for the conduction of tissue regeneration: engineering cell-invasion characteristics. *Proc Natl Acad Sci U S A.* 2003;100(9):5413-5418.

60. West JL, Hubbell JA. Polymeric biomaterials with degradation sites for proteases involved in cell migration. *Macromolecules.* 1999;32:241-244.

61. van de Wetering P, Metters AT, Schoenmakers RG, Hubbell JA. Poly(ethylene glycol) hydrogels formed by conjugate addition with controllable swelling, degradation, and release of pharmaceutically active proteins. *J Control Release.* 2005;102(3):619-627.

62. Schoenmakers RG, van de Wetering P, Elbert DL, Hubbell JA. The effect of the linker on the hydrolysis rate of drug-linked ester bonds. *J Control Release.* 2004;95(2):291-300.

63. Jo S, Shin H, Fisher JP, Mikos AG. Synthesis and characterization of oligo(poly(ethylene glycol) fumarate) macromer. *Macromolecules.* 2001;34:2839-2844.

64. Reddy SK, Anseth KS, Bowman CN. Modeling of network degradation in mixed step-chain growth polymerization. *Polymer.* 2005;46(12):4212-4222.

65. Park KH, Na K, Chung HM. Enhancement of the adhesion of fibroblasts by peptide containing an Arg-Gly-Asp sequence with poly(ethylene glycol) into a thermo-reversible hydrogel as a synthetic extracellular matrix. *Biotechnology letters.* 2005;27(4):227-231.

66. Salinas CN, Cole BB, Kasko AM, Anseth KS. Chondrogenic differentiation potential of human mesenchymal stem cells photoencapsulated within poly(ethylene glycol)-arginine-glycine-aspartic acid-serine thiol-methacrylate mixed-mode networks. *Tissue engineering.* 2007;13(5):1025-1034.

67. Shu XZ, Ghosh K, Liu Y, Palumbo FS, Luo Y, Clark RA, Prestwich GD. Attachment and spreading of fibroblasts on an RGD peptide-modified injectable hyaluronan hydrogel. *Journal of biomedical materials research.* 2004;68(2):365-375.

68. Nuttelman CR, Tripodi MC, Anseth KS. Synthetic hydrogel niches that promote hMSC viability. *Matrix Biol.* 2005;24(3):208-218.

69. Weber LM, Hayda KN, Haskins K, Anseth KS. The effects of cell-matrix interactions on encapsulated beta-cell function within hydrogels functionalized with matrix-derived adhesive peptides. *Biomaterials.* 2007;28(19):3004-3011.

70. Canal T, Peppas NA. Correlation between mesh size and equilibrium degree of swelling of polymeric networks. *J Biomed Mater Res.* 1989;23(10):1183-1193.

71. Buxton AN, Zhu J, Marchant R, West JL, Yoo JU, Johnstone B. Design and characterization of poly(ethylene glycol) photopolymerizable semi-interpenetrating networks for chondrogenesis of human mesenchymal stem cells. *Tissue engineering.* 2007;13(10):2549-2560.

72. Cruise GM, Scharp DS, Hubbell JA. Characterization of permeability and network structure of interfacially photopolymerized poly(ethylene glycol) diacrylate hydrogels. *Biomaterials.* 1998;19(14):1287-1294.

73. Rydholm AE, Held NL, Benoit DS, Bowman CN, Anseth KS. Modifying network chemistry in thiol-acrylate photopolymers through postpolymerization functionalization to control cell-material interactions. *Journal of biomedical materials research.* 2007. *Epub ahead of print*.

74. Yang PJ, Temenoff JS. Effect of tethered RGD on stem cell retention in fumarate hydrogels. *Society for Biomaterials 8th World Congress*. Amsterdam, The Netherlands; 2008.

75. Bryant SJ, Anseth KS. Controlling the spatial distribution of ECM components in degradable PEG hydrogels for tissue engineering cartilage. *Journal of biomedical materials research.* 2003;64(1):70-79.

76. Benjamin M, Ralphs JR. Tendons and ligaments--an overview. *Histology and histopathology.* 1997;12(4):1135-1144.

77. Pedrosa-Domellof F, Tiger CF, Virtanen I, Thornell LE, Gullberg D. Laminin chains in developing and adult human myotendinous junctions. *J Histochem Cytochem.* 2000;48(2):201-210.

78. Benjamin M, Ralphs JR. The cell and developmental biology of tendons and ligaments. *International review of cytology.* 2000;196:85-130.

79. Battistelli M, Borzi RM, Olivotto E, Vitellozzi R, Burattini S, Facchini A, Falcieri E. Cell and matrix morpho-functional analysis in chondrocyte micromasses. *Microscopy research and technique.* 2005;67(6):286-295.

80. Xu Y, Balooch G, Chiou M, Bekerman E, Ritchie RO, Longaker MT. Analysis of the material properties of early chondrogenic differentiated adipose-derived stromal cells (ASC) using an in vitro three-dimensional micromass culture system. *Biochemical and biophysical research communications.* 2007;359(2):311-316.

81. Yang JW, de Isla N, Huselstein C, Sarda-Kolopp MN, Li N, Li YP, Jing-Ping OY, Stoltz JF, Eljaafari A. Evaluation of human MSCs cell cycle, viability and differentiation in micromass culture. *Biorheology.* 2006;43(3-4):489-496.